NMRI-97-38

TOXICOLOGY DETACHMENT

THE PHYSICOCHEMICAL PROPERTIES OF SFE FIRE SUPPRESSANT ATMOSPHERES IN TOXICITY vs FIRE EXTINGUISHMENT TESTS: IMPLICATIONS FOR AEROSOL DEPOSITION AND TOXICITY

E.C. Kimmel
E.A. Smith
J.E. Reboulet
K.R. Still
R.L. Carpenter

NOVEMBER 1997

INTERIM REPORT FOR PERIOD NOVEMBER 1995 - OCTOBER 1997

Approved for public release; distribution is unlimited

NAVAL MEDICAL RESEARCH INSTITUTE
WRIGHT-PATTERSON AIR FORCE BASE, OHIO 45433-7094

NOTICES

When U.S. Government drawings, specifications. Or other data are used for any purpose other than a definitely related Government procurement operation, the Government thereby incurs no responsibility nor any obligation whatsoever, and the fact that the Government may have formulated, furnished, or in any way supplied the said drawings, specifications, or other data, is not to be regarded by implication or otherwise, as in any manner licensing the holder or any other person or corporation, or conveying any rights or permission to manufacture, use, or sell any patented invention that may in any way be related thereto.

Please do not request copies of this report from the Naval Medical Research Institute Detachment (Toxicology). Additional copies may be purchased from:

National Technical Information Service
5285 Port Royal Road
Springfield, Virginia 22161

Federal Government agencies and their contractors registered with Defense Technical Information Center should direct requests for copies of this report:

Defense Technical Information Center
Cameron Station
Alexandria, Virginia 22314

TECHNICAL REVIEW AND APPROVAL
NMRI-97-38

The experiments reported herein were conducted according to the "Guide for the Care and Use of Laboratory Animals," Institute of Laboratory Animal Resources, National Research Council

This report has been reviewed by the Office of Public Affairs (PA) and is releasable to the National Technical Information Service (NTIS). At NTIS, it will be available to the general public, including foreign nations.

This technical report has been reviewed and is approved for publication.

FOR THE COMMANDING OFFICER

KENNETH R. STILL, CAPT, MSC, USN
Officer-in-Charge
Naval Medical Research Institute Detachment (Toxicology)

REPORT DOCUMENTATION PAGE

Form Approved
OMB No. 0704-0188

1. AGENCY USE ONLY *(Leave blank)*	2. REPORT DATE	3. REPORT TYPE AND DATES COVERED
	November 1997	November 1995 - October 1997

4. TITLE AND SUBTITLE
The Physicochemical Properties of SFE Fire Suppressant Atmospheres in Toxicity vs Fire Extinguishment Tests: Implications for aerosol deposition and toxicity

5. FUNDING NUMBERS
REIMB.NAVSEA.1430

6. AUTHOR(S)
E.C. Kimmel, E.A. Smith, J.E. Reboulet, R.L. Carpenter, K.R. Still

7. PERFORMING ORGANIZATION NAME(S) AND ADDRESS(ES)
Naval Medical Research Institute Detachment Toxicology
NMRI/TD
2612 Fifth Street, Building 433
Area B
Wright-Patterson AFB, OH 45433-7094

8. PERFORMING ORGANIZATION REPORT NUMBER

9. SPONSORING/MONITORING AGENCY NAME(S) AND ADDRESS(ES)
Naval Medical Research Institute Detachment Toxicology
NMRI/TD
2612 Fifth Street, Building 433
Area B
Wright-Patterson AFB, OH 45433-7094

10. SPONSORING/MONITORING AGENCY REPORT NUMBER
NMRI-97-38

11. SUPPLEMENTARY NOTES

12a. DISTRIBUTION AVAILABILITY STATEMENT
Approved for public release; distribution is unlimited.

12b. DISTRIBUTION CODE

13. ABSTRACT *(Maximum 200 words)*

Comparisons were made between the physicochemical properties of Spectronics Fire Extinguishant (SFE) atmospheres generated either in a fire extinguishment or inhalation toxicity assessment regimen. Aerosol and gas phase components in the atmospheres were dynamic as opposed to steady-state, hjaving varying rates concentration change. Fire extinguishment test conditions closely approximate those proposed for deployment of SFE as a fire extinguishing agent. Significant differences in aerosol mass concentration, size distribution and shifts in size distribution were found between the two types of atmospheres, eachgenerated at two comparable target (nominal) concentrations. Likewise, differences in CO2 and CO concentration and dissipation rates of these gases also were found between the two types of atmospheres. A series of theoretical calculations of CO2 induced hypercapnea were developed as a basis to examine possible interaction of the components of the atmospheres. A hypotehetical case for aerosol deposition rate and carboxyhemoglobin formation and changes in the rrates of these phenomena was formulated for each atmosphere. These cases accounted for component interaction effects on potential toxicity. For ease of comparison of these hypothetical cases, 3-dimentianal graphics were used to ilustrate the magnitude of the relative differences in particle deposition and carboxyhemoglobin formation between the atmospheres. Data from corresponding animalstudies have beenpublished clearly demonstrate pulmonry toxicity in rats from exposure to the high target load SFE atmosphere in the toxicity testing system. SFE atmospheres as generated in the fire extinguishment testing regimen wre found to have greater potential toxicity than those generated in the toxicity testing system.

14. SUBJECT TERMS
Fire Extinguishment, Aerosol, Deposition, Carboxyhemoglobin

15. NUMBER OF PAGES
48

16. PRICE CODE

17. SECURITY CLASSIFICATION OF REPORT	18. SECURITY CLASSIFICATION OF THIS PAGE	19. SECURITY CLASSIFICATION OF ABSTRACT	20. LIMITATION OF ABSTRACT
UNCLASSIFIED	UNCLASSIFIED	UNCLASSIFIED	UL

GENERAL INSTRUCTIONS FOR COMPLETING SF 298

The Report Documentation Page (RDP) is used in announcing and cataloging reports. It is important that this information be consistent with the rest of the report, particularly the cover and title page. Instructions for filling in each block of the form follow. It is important to ***stay within the lines*** to meet ***optical scanning requirements.***

Block 1. Agency Use Only *(Leave blank)*.

Block 2. Report Date. Full publication date including day, month, and year, if available (e.g. 1 Jan 88). Must cite at least the year.

Block 3. Type of Report and Dates Covered. State whether report is interim, final, etc. If applicable, enter inclusive report dates (e.g. 10 Jun 87 - 30 Jun 88).

Block 4. Title and Subtitle. A title is taken from the part of the report that provides the most meaningful and complete information. When a report is prepared in more than one volume, repeat the primary title, add volume number, and include subtitle for the specific volume. On classified documents enter the title classification in parentheses.

Block 5. Funding Numbers. To include contract and grant numbers; may include program element number(s), project number(s), task number(s), and work unit number(s). Use the following labels:

C - Contract	**PR** - Project
G - Grant	**TA** - Task
PE - Program Element	**WU** - Work Unit Accession No.

Block 6. Author(s). Name(s) of person(s) responsible for writing the report, performing the research, or credited with the content of the report. If editor or compiler, this should follow the name(s).

Block 7. Performing Organization Name(s) and Address(es). Self-explanatory.

Block 8. Performing Organization Report Number. Enter the unique alphanumeric report number(s) assigned by the organization performing the report.

Block 9. Sponsoring/Monitoring Agency Name(s) and Address(es). Self-explanatory.

Block 10. Sponsoring/Monitoring Agency Report Number. *(If known)*

Block 11. Supplementary Notes. Enter information not included elsewhere such as: Prepared in cooperation with....; Trans. of....; To be published in.... When a report is revised, include a statement whether the new report supersedes or supplements the older report.

Block 12a. Distribution/Availability Statement. Denotes public availability or limitations. Cite any availability to the public. Enter additional limitations or special markings in all capitals (e.g. NOFORN, REL, ITAR).

- **DOD** - See DoDD 5230.24, "Distribution Statements on Technical Documents."
- **DOE** - See authorities.
- **NASA** - See Handbook NHB 2200.2.
- **NTIS** - Leave blank.

Block 12b. Distribution Code.

- **DOD** - Leave blank.
- **DOE** - Enter DOE distribution categories from the Standard Distribution for Unclassified Scientific and Technical Reports.
- **NASA** - Leave blank.
- **NTIS** - Leave blank.

Block 13. Abstract. Include a brief *(Maximum 200 words)* factual summary of the most significant information contained in the report.

Block 14. Subject Terms. Keywords or phrases identifying major subjects in the report.

Block 15. Number of Pages. Enter the total number of pages.

Block 16. Price Code. Enter appropriate price code *(NTIS only)*.

Blocks 17. - 19. Security Classifications. Self-explanatory. Enter U.S. Security Classification in accordance with U.S. Security Regulations (i.e., UNCLASSIFIED). If form contains classified information, stamp classification on the top and bottom of the page.

Block 20. Limitation of Abstract. This block must be completed to assign a limitation to the abstract. Enter either UL (unlimited) or SAR (same as report). An entry in this block is necessary if the abstract is to be limited. If blank, the abstract is assumed to be unlimited.

PREFACE

This is one of a series of technical report describing results of the experimental laboratory programs conduced at the Naval Medical Research Institute Detachment (Toxicology). This document serves as a interim report on The Physicochemical Properties of SFE Fire Suppressant Atmospheres in Toxicity vs. Fire Extinguishment Tests: Implications for aerosol deposition and toxicity. The research described in this report began in November 1995 and was completed in October 1997 under Navy Contract No. REIMB.NAVSEA.1430. This study was sponsored by the U.S. Navy under the direction of CAPT Kenneth R. Still, MSC, USN.

The opinions contained herein are those of the authors and are not to be construed as official or reflecting the view of the Department of the navy or the Naval Services at large.

TABLE OF CONTENTS

ABSTRACT

Comparisons were made between the physicochemical properties of Spectronics Fire Extinguishant (SFE) atmospheres generated either in a fire extinguishment or inhalation toxicity assessment regimen. Aerosol and gas phase components in the atmospheres were dynamic as opposed to steady-state, having varying rates concentration change. Fire extinguishment test conditions closely approximate those proposed for deployment of SFE as a fire extinguishing agent. Significant differences in aerosol mass concentration, size distribution and shifts in size distribution were found between the two types of atmospheres, each generated at two comparable target (nominal) concentrations. Likewise, differences in CO_2 and CO concentration and dissipation rates of these gases also were found between the two types of atmospheres. A series of theoretical calculations of CO_2 induced hypercapnea were developed as a basis to examine possible interaction of the components of the atmospheres. A hypothetical case for aerosol deposition rate and carboxyhemoglobin formation and changes in the rates of these phenomena was formulated for each atmosphere. These cases accounted for component interaction effects on potential toxicity. For ease of comparison of these hypothetical cases, 3-dimentional graphics were used to illustrate the magnitude of the relative differences in particle deposition and carboxyhemoglobin formation between the atmospheres. Data from corresponding animal studies have been published clearly demonstrate pulmonary toxicity in rats from exposure to the high target load SFE atmosphere in the toxicity testing system. SFE atmospheres as generated in the fire extinguishment testing regimen were found to have greater potential toxicity than those generated in the toxicity testing system.

KEY WORDS

fire extinguishment, aerosol, deposition, carboxyhemoglobin

Acknowledgements/Disclaimer

This research was sponsored by the Navy CFC/Halon Replacement Program; NAVSEASYSCOM Code 03V2 and conducted atn the Naval Medical Research Institute Detachment (Toxicology). The authors wish to thank Petty Officer C. Alva for his assistance with this project. Opinions contained herein are those of the authors and are not to be construed as official or as reflecting the view of the Department of the Navy or the Naval Service at large. Mention of commercial products or services does not constitute endorsement by the Department of the Navy or the Naval Service at large.

LIST OF ABBREVIATIONS

Note common chemical and measurement abbreviations are not included.

AWG	American Wire Gauge
SFE	Spectronix Fire Extinguishant
NMRI/TD	Naval Medical Research Institute Detachment (Toxicology)
NRL/CBD	Naval Research Laboratory/Chesapeake Bay Detachment
MMAD	Mass Median Aerodynamic Diameter
σg	Geometric Standard Deviation
NIST	National Institute of Standards and Technology
APS	Aerodynamic Particle Sizer
SSA	Specific Surface Area
RH	Relative Humidity
TR	Total Respiratory Tract
TB	Tracheobronchial region
P	Pulmonary region
NP	Nasophryngeal region
ICRP	International Commission on Radiation Protection
R	Respiratory Quotient or Respiratory Exchange Ratio
$\dot{V}$	Volumetric flow
Ve	Minute Ventilation
$PAco_2$	Alveolar Partial Pressure of Carbon Dioxide
PAo_2	Alveolar Partial Pressure of Oxygen
COHb	Carboxyhemoglobin

LIST OF TABLES

LIST OF FIGURES

INTRODUCTION

Spectronix Fire Extinguishant (SFE) is a dry powder aerosol type fire suppressant which is under investigation by the Naval Research Laboratory (NRL) as a replacement for ozone depleting Halons currently used in total flooding type fire extinguishment systems. The efficacy of SFE as a fire extinguishing agent has been reported [1,2,3]. These tests were conducted in a 56 m^3 compartment well suited for fire suppression studies located at NRL's Chesapeake Bay Detachment (NRL/CBD). SFE aerosols, which are generated pyrotechnically from bulk solid, were tested at two nominal aerosol concentrations of 50 and 80 g/m^3. However during these previous fire extinguishment tests no measurements of actual aerosol mass concentration and particle size distribution were made. Hence the respirability of the SFE aerosols was not determined. Prior to deployment of SFE it was necessary to evaluate the potential inhalation toxicity of this material. Consequently, a series of inhalation toxicity studies were undertaken by the Naval Medical Research Institute Detachment (Toxicology) - (NMRI/TD) using a 0.7 m^3 inhalation exposure chamber[4]. Although the basic pyrotechnic technique for SFE atmosphere generation was the same in the two test systems, there were significant operational differences between the test systems which warranted a thorough characterization and comparison of the SFE atmospheres generated at comparable nominal concentrations.

SFE pyrolysis is self perpetuating and produces transient pressure and thermal pulses, which obfuscate inhalation toxicity evaluations. Thus, for toxicity evaluations a system was designed in which the SFE was ignited in one portion of the system for rapid dissipation of the pressure and thermal pulse and the combustion atmosphere produced then transported into a whole body inhalation exposure chamber. This procedure differs from the fire extinguishment testing scenario used at NRL/CBD in which SFE was ignited within the test chamber itself. A procedure which more closely simulates actual SFE deployment methods and conditions. SFE atmospheres in both test systems were dynamic with concentrations of all principal constituents and size distribution of the aerosol phase changing with time. However, the relative magnitude and proportion of the principal constituents in the atmospheres and the rates at which atmosphere composition changes differ between the two test systems. The differing dynamic behavior of the atmospheres complicates comparison of the potential toxicity of the atmospheres, primarily because the atmospheric constituents interact with a synergistic effect on potential toxicity.

Theoretical mathematical descriptions of atmosphere constituent interaction and 3-dimentional graphic techniques were developed to illustrate the effect of differing constituent kinetics and interactions on potential aerosol deposition and carboxyhemoglobin formation in humans. The 3-dimentional plots were used as a simplified method by which to compare the potential toxicity of these complex atmospheres.

METHODS

Test Material

The SFE (Formulation A) tested in both systems was obtained from the Spectrex, Inc., the U.S. subsidiary of an Israeli company - Spectronix, Ltd. The composition of SFE is proprietary.

Atmosphere (Aerosol) Generation

The aerosol generators used in the 56 m^3 chamber test system have been previously described in detail (2). The aerosol generator used in the 0.7 m^3 test system was manufactured out of two sections of 7.62 cm diameter schedule 80 stainless steel pipe (**Figure 1**). The lower ($h \cong 7.6$ cm) and upper ($h \cong 20.3$ cm) sections of pipe were connected by flanges. A stainless steel fritted metal plate (0.3 cm thick) was placed between the flanges. The lower section included an 0.32 cm compression fitting through which 31 L/min air flow was metered using a rotameter (Matheson Gas Products, Twinsburg, OH). The air flow facilitated transport of the SFE combustion atmosphere to the exposure chamber. The upper section of the generator was fitted with 0.16 cm compression fitting to hold a Pr/Rh thermocouple (# 8720, Omega Engineering, Stamford, CT) for recording generator temperature during SFE ignition. A 2.54 cm diameter compression fitting in the upper section held an igniter assembly which consisted of a 2.54 cm diameter x 6.35 cm phenolic rod pierced with two 0.32 cm diameter electrodes. A folded length of chromel A, nichrome wire (26 AWG, Hoskins Mfg. Co., Hamburg, MI) sufficient to yield a 3 ohm resistance ($\cong$ 28 cm) was attached to the interior ends of the electrodes. Ignition current (6 amps - 4 watts/cm) was provided by a 115 v power source through a 115 to 18 v step-down transformer (Triad Transformer Co., Los Angeles, CA) with leads attached to the exterior ends of the igniter electrodes. The folded igniter wire was placed in a 5 cm diameter ceramic boat (#60050, Coors Ceramicon Designs, Ltd., CO) located in the bottom of the upper plenum (on the fritted plate). A pre-weighed piece of SFE was placed directly on

directly on the igniter wire. The loaded generator assembly was connected via threaded fittings to 6.35 cm diameter aluminum duct (total length ≅ 2.5 m) which served as conduit to the exposure chamber inlet. The SFE was ignited by applying 115 v power to the transformer. An ignition temperature for SFE of ≅ 500 °C was attained by the igniter assembly within a few seconds, and combustion of the SFE (depending on total mass ignited) was complete within ≅ 15 seconds. Although temperature in the generator assembly reached 1100 ± 100 °C the generator assembly and the aluminum duct acted as a heat sink so that the exposure chamber temperature was elevated by less than 2 °C (initial 22 to 24 °C) for ≅ 5 min.

Test Chambers

The 0.7 m^3 inhalation exposure chamber was not operated in the dynamic (continuous flow) mode that is routinely used for inhalation exposures (**Figure 2**). For this investigation the chamber was operated in the static (non-flowing) mode that is generally used for single event atmosphere generation such as occurs by combustion. During generation, the SFE atmospheres were piped into the chamber in the dynamic mode of operation; once combustion was complete the chamber was switched to the static mode via automatic shut-off valves at the inlet and exhaust ports. A sight glass fitted into the chamber inlet duct enabled visual determination of cessation of SFE pyrolysis and completion of transport. Automated control of system flow and pressure differential assisted chamber filling with inconsequential loss of test atmosphere through the chamber exhaust, and rapid dissipation of the generation pressure pulse. Generator and chamber flow during ignition and filling was 30 - 31 L/min. and chamber filling time ranged from 0.75 to 1.0 min. at which point static operation was initiated. Chamber exhaust flow was provided by a water-misting scrubber (Model HSB-30, Heat Systems Ultrasonics Inc., Farmingdale NY). Prior to ignition the exhaust flow and inlet flows were balanced so that the exposure chamber was maintained at a sub-ambient pressure of 10.16 to 15.24 cm H_20 subambient. At the end of each 1 hr test period the chamber was reverted to dynamic operation; the chamber inlet flow was diverted from the generator assembly to a passive inlet port so that the chamber could be rapidly evacuated at a high flow (≅ 220 L/min). Chamber pressure during this maneuver was 0.25 to 0.5 cm H_2O subambient. Complete evacuation of the test atmosphere was accomplished within 9 min.

The 56 m^3 chamber has been described previously (1).

Aerosol Analysis

Identical analytical methods were used in both test systems for characterization of the aerosol component of the SFE atmospheres. Aerosol mass concentration was determined by gravimetric analysis of particles collected on 37 mm diameter glass fiber filters (Model 61631, Gelman Sciences, Ann Arbor, MI) placed in holders specifically designed for aerosol sampling (Intox Products, Albuquerque, NM) through which a known volume of test atmosphere was drawn. Sample flow was measured and controlled with variable area rotameters (Matheson Gas Products, Twinsburg, OH) calibrated to National Institute for Standards and Testing (NIST) traceable standards. Sample volume was controlled by electronic timing (Model 645, Gralab Instruments Division, Centerville, OH) of solenoid valves in the sample lines. Flows and subsequently sample volumes were adjusted for changes in pressure differential across the sampling device. In the 0.7 m^3 chamber, samples were drawn through 1.2 cm dia. sample probes penetrating the chamber wall. Sample velocity and probe design allowed nearly isokinetic, non-turbulent sample flow which eliminated sample probe aerosol deposition and sampling velocity artifact. In the 56m^3 chamber, the filter holders were located directly within the chamber at the end of separate vacuum lines. Shutoff valves in each of these lines were connected to manifold so that a single calibrated flow source could be used for sampling. The sample volumes were controlled in the same manner as described for the 0.7 m^3 chamber sampling system. Filter samples were collected at 1, 15, 30, and 60 min. in the 0.7 m^3 chamber and at 1.5, 15, 30 and 60 min. in the 56 m^3 chamber. To prevent chamber depressurization an automated valve system was used to inject flows equivalent to the sampling flow into the exhaust manifold of the 0.7 m^3 chamber during sampling. Reported concentrations have been adjusted for loss of mass concentration due to previous sample collection.

Mass median aerodynamic diameter (MMAD) and the geometric standard deviation (σg) of the aerosol distribution were determined by two methods. Eight stage, multi-jet cascade impactors (Intox Products, Albuquerque, NM) were used to collect samples for gravimetric analysis at time points corresponding to filter sample collections. Sample flows and pressure differentials were controlled in a manner similar to filter samples. In the 56 m^3 chamber the impactors also were located within the chamber at the terminus of individual vacuum lines. A

ball valve assembly similar to that used for large chamber filter sampling was for collection of the impactor samples.

Aerosol size distribution characteristics also were determined using a laser, time of flight, individual particle analyzer {Model 3300B Aerodynamic Particle Sizer (APS), TSI, Inc., St. Paul, MN}. The APS was capable of separating the particle distribution into 58 individual size ranges from 0.47 to 30.0 μm diameter particles, thus allowing for a much greater resolution of the particle size distribution. APS samples were drawn through two diluters (Model 3302, TSI, Inc., St. Paul, MN) in series for a 10,000:1 dilution. Flow splitting methods were employed to provide a total dilution of 40,000:1 necessary to prevent nozzle clogging and to minimize coincidence loss in the APS (**Figure 3**). Comparative analysis of diluted and undiluted samples (of short duration) by cascade impaction methods demonstrated that the dilution procedures did not significantly alter aerosol size distribution. APS samples were taken at 1 or 1.5, 15, 30, 45, and 60 min. MMAD and σg determinations were based on impactor samples, whereas changes in aerosol distribution shape and modality were based on APS samples.

Gas Analysis

Chromatographic methods were used for CO_2 analysis at the NRL/CBD test site (56 m^3 chamber) and have been described previously[2]. Carbon monoxide concentration in the 56 m^3 chamber was measured continuously by wavelength-specific, non-dispersive IR spectrometry (Enviromax 3000, Liston Scientific, Irvine, CA). Wave-length-specific, non-dispersive IR spectrometry was used for both CO and CO_2 in the 0.7 m^3 chamber (Model 865 Beckman Industries, La Habra, CA). The latter samples were collected at times corresponding to APS samples. Electro-chemical measurement of O_2 concentration in the 56 m^3 chamber was continuous (Enviromax 3000) and on a grab sample basis in the 0.7 m^3 chamber (Model 326RA, Teledyne Analytical Instruments, City of Industry, CA). Gas sampling systems for the 0.7 m^3 chamber were similar to the aerosol sampling systems, each having a corresponding balanced make up air return to the chamber exhaust line to prevent chamber depressurization during sampling. Gas sample volumes removed from the large test chamber were inconsequential and adjustment of samples to correct prior sampling artifact was not required.

Particle Morphology

An electrostatic precipitator (Model 02-1500, Intox Products, Albuquerque NM) was used to collect particles for examination by scanning and transmission electron microscopy to determine aerosol particle morphology and composition by X-ray defraction. Multistage cyclone samples were collected for analysis of particle specific surface area (SSA) and particle density by Braunuer-Emmitt-Teller analysis of N_2 adsorption isotherms[5] using an adsorption analyzer (Quantasorb, Quantachrome Inc., Boynton Beach, FL).

Experimental Design

All test periods were 60 minutes. The test schedule is shown in **Table 1**.

RESULTS

Spatial Distribution - 56 m^3 chamber

The 0.7 m^3 inhalation exposure chamber was specifically designed for mixing and even distribution of aerosols within the chamber exposure volume; chamber characterization has been reported elsewhere[4]. In the large chamber, mixing and dispersal of the aerosol was accomplished by using a fan during the first 1.5 min. after ignition of the SFE. A single trial was made at the 50 g/m^3 target load to determine spatial variation within the chamber of aerosol concentration, size distribution and CO_2 concentration. Measurements were made over the course of 1 hr at heights of 0.3, 1, 1.75 and 3.3 m and at distances of approximately 2.0 m from the left and rear walls of the chamber. No significant differences of spatial or temporal distribution of either the aerosol or CO_2 components of the SFE atmospheres were found in the 56 m^3 chamber (**Tables 2 and 3**).

Aerosol Mass Concentration

Initial, actual aerosol mass concentration for both target loads, 50 and 80 g/m^3, was higher in 56 m^3 chamber at 10.2 and 14 g/m^3 respectively vs. 6.3 and 10.0 g/m^3 respectively for the 0.7 m^3 chamber. Gravitational settling of particles throughout the test period resulted in final concentrations of 1.7 and 1.2 g/m^3 in the 50 and 80 g/m^3 loads in the 56 m^3 chamber. Final aerosol concentrations in the 0.7 m^3 chamber were 0.7 g/m^3 for both loads (**Figure 4**). In both chambers and for both target loads, decay of aerosol concentration was exponential. Shorter half-times ($T_{1/2}$) of 15.5 and 16.1 min. were found for the higher target load for the 0.7 and 56 m^3 chambers respectively. $T_{1/2}$ for the low target load was 18.6 and 22.4 min. respectively.

Aerosol Size Distribution and Particle Growth

The initial MMADs for the four atmospheres ranged from 2.4 to 3.0 μm , maximum MMADs ranged from 3.0 to 6.3 μm. The σgs of the particle distributions ranged from 1.42 to 2.01 at various times; however, average σgs were 1.66 to 1.88. Growth was more rapid for the higher target load in both chambers and apparently much more rapid in the 56 m^3 chamber (**Figure 5**).

CO and CO_2 Concentration

CO_2 concentrations in the 56m^3 chamber were much higher at both target loads than corresponding concentrations in the 0.7 m^3 chamber. The large chamber was not a well-sealed, containment vessel as are inhalation exposure chambers; therefore, in this chamber the gas phase components of the SFE atmospheres underwent concentration decay similar to that of the aerosol phase. Initial CO_2 concentrations for the 50 and 80 g/m^3 loads in the large chamber were 14,475 and 22,200 ppm respectively. Final CO_2 concentrations for the large chamber were 7,100 and 9,500 ppm respectively. CO_2 concentrations in the 0.7 m^3 chamber were steady-state at 10,230 to 10,105 ppm for the 50 g/m^3 target load. CO_2 concentrations for the 80 g/m^3 load in the 0.7 m^3 chamber were 9,457 ppm initially to 9,376 ppm at 60 min (**Figure 6**). Initial and final CO concentrations in the 0.7 m^3 chamber were 2,168 and 2,538 ppm at the 50 g/m^3 load. At the 80 g/m^3 load initial and final CO concentrations were 6,548 and 6,360 ppm respectively in the 0.7 m^3 chamber. In the 56 m^3 chamber long sampling lines and a large dead space (in-line filter assembly required to remove particles from the sample) in the CO analysis system lead to large sample lag time (≅ 20 min.). Consequently, CO concentration measurements that did not include sample system artifact were not obtained until the 20 min sample point. Known sampling delays were factored into CO concentration vs. time analysis. Carbon monoxide concentrations were fitted to an exponential decay curve comparable to those observed for CO_2 . Decay rate constants for the CO concentration curves were calculated by adjusting corresponding CO_2 decay constants in proportion to the diffusion coefficient ratio for these gases. Diffusion was assumed to be the predominant factor in gas concentration decay. Gas diffusion coefficient ratio was determined by Graham's law[6] . Maximum observed CO concentrations in the 56 m^3 chamber were, for the 50 and 80 g/m^3 loads respectively, 2,992 and 4,810 ppm, whereas extrapolated peak CO concentrations were estimated to be 5,485 and 10,148 ppm respectively (**Figure 7**). Oxygen

concentration in the 56 m^3 varied from 19.1 to 19.9 % and ranged from 20.1 to 20.6 % in the 0.7 m^3 chamber.

Particle Morphology

Energy dispersive X-ray analysis indicated that SFE aerosol particles were composed of greater than 97 % KCl, with traces of a variety of metals and KOH[7]. The SSA of particles from the 0.7 m^3 chamber at the low target load was 2.74 m^2/g and particle density was determined to be 2.23 g/cm^3 . These were comparable to a predicted value of SSA = 2.08 m^2/g for 3.3 μm MMAD (average over of all samples) spherical particles and an assuming particle density equivalent to the bulk density of KCl[8], 1.98 g/cm^3 . This indicated that the individual (non-agglomerated) aerosol particles were not cenospherical and were slightly porous. Electron microscopy of particles showed that individual particles and agglomerate particles in the 0.7 m^3 chamber atmospheres were cubiodal crystals. Particles and agglomerates collected from 56 m^3 chamber atmospheres were spherical with evidence of surface remodeling due to moisture. The relative humidity (RH) in the 56 m^3 chamber during the testing period was at or near 100 % compared to an average 30 % RH in the 0.7 m^3 chamber atmospheres.

DISCUSSION

Systems Mass Balance and Comparative Efficiencies

Mass balance calculations, based on peak concentrations, indicate that in the 0.7 m^3 chamber test system 10.7 and 23.4 % of the mass of SFE ignited, for the 50 and 80 g/m^3 loads, remained unaccounted for by the aerosol , CO_2 and CO yields. At target concentrations of 50 and 80 g/m^3, 24.8 and 25 % of the SFE ignited, respectively, remained unaccounted for in the 56 m^3 chamber. The 0.7 m^3 system used bulk SFE more efficiently than its 56 m^3 counterpart at the lower target concentration. However, with respect to aerosol generation 12.3 and 12.4 % of the SFE mass was aerosolized at the 50 and 80 g/m^3 loads in the 0.7 m^3 chamber; whereas aerosolization was 19 and 17.4 % of the SFE mass at the 50 and 80 g/m^3 loads in the 56 m^3 chamber. The average ratio (both target loads) of aerosol formation efficiency in the chambers was 1.5:1 (56:0.7 m^3 chambers) . Therefore, the large system was 50 % more efficient at aerosol dispersal if not formation. A slightly greater overall efficiency for pyrolysis of SFE for the 0.7 m^3 chamber system suggested that transport loss of aerosol and not aerosol production was the

cause for the observed difference in aerosol dispersion efficiency. CO_2 concentration in the 0.7 m^3 system was greater at the lower target load than at the higher target load, suggesting that combustion efficiency in the generator was greater at the lower target concentration. Consequently the mass percentages of CO_2 yield were not similar, at 38.2 and 21.8 %, for the 50 and 80 g/m^3 loads respectively. Yields of CO_2 (using peak concentrations) in the 56 m^3 chamber were similar at 49.6 and 50.6 % for the 50 and 80 g/m^3 loads. The relative CO_2 production ratio, based on peak mass concentration, for the systems (56:0.7 m^3 chambers) was 2.1:1 at the 50 g/m^3 load and 1.5:1 at the 80 g/m^3 load. CO production (using extrapolated peak values) accounted for 11.9 and 14.6 % of the SFE mass used in the 56 m^3 chamber at the 50 and 80 g/m^3 loads respectively. CO yield in the 0.7 m^3 system was 6.5 and 6.9 % for the 50 and 80 g/m^3 loads respectively. CO production ratio, based on peak and estimated peak mass concentrations, for the systems (56:0.7 m^3 chambers) was 1.8:1at 50.0 g/m^3 and 2.1:1 at 80 g/m^3 targets. These ratios suggest that the SFE combustion process for both systems was not complete regardless of target load and that, overall, combustion efficiency in the fire extinguishment test system was greater than that of the inhalation toxicity test system.

Particle Growth

For aerosols with $\cong$ 3.0 μm MMADs and σgs of 1.7, having the high initial mass concentrations observed in the study of 14, 10.2, 10.0 and 6.3 g/m^3 have corresponding particle number concentrations of 1.78×10^6, 1.30×10^6, 1.27×10^6 and 0.8×10^6 particles/cm^3, assuming an SFE particle density of $\approx$2.0 g/cm^3. Aerosols with a number concentration of 1.0×10^6 particles/cm^3 have a theoretical number concentration $T_{1/2}$ of $\cong$ 33 min. due to coagulation and agglomeration, assuming no depletion of total aerosol mass due to settling[8,9]. Consequently, it was assumed that coagulation was a primary factor in the observed particle growth and in the differences in particle growth at the respective target loads. Salt aerosol particles are known to be very hygroscopic and subject to rapid growth at a characteristic RH (84 % for KCl) at which particle dissolution occurs[10]. The apparent increase in particle growth found in the 56 m^3 chamber is most likely due to an initial rapid hygroscopic growth at RH $\cong$ 100% coupled with coagulation.

Potential Toxicity - Aerosol Deposition and Carboxyhemoglobin Formation

There are several possible untoward effects implicit in the inhalation of atmospheres of SFE, however only particle deposition and formation of carboxyhemoglobin will be addressed.

Particle Growth Effects

Based on the current International Commission on Radiation Protection human particle deposition curves[11] the particle growth observed in all experimental conditions would increase total respiratory tract deposition (TR). The 1 μm increase in MMAD in the 0.7 m^3 chamber seen for both the 50 and 80 g/m^3 loads correspond to increases in total lung deposition of 5 and 3 %. In the 56 m^3 chamber, the 2 μm increase of MMAD would result in a 7 % increase in TR while an increase of 3.9 μm at the 80 g/m^3 load would result in a 20 % increase in TR. Particle growth-induced deposition changes would be greater for the various subcompartments of TR because of the greater dependence of regional deposition on particle size. In the naso-oro-pharyngeal (NP) region, particle deposition would increase by as little as 8 % (0.7 m^3 - 80 g/m^3) to as much as 45 % (56 m^3 - 80 g/m^3). Tracheobronchial (TB) region deposition, based on curves developed by Cheng and Yeh[12], would increase by 6 % at either target load in the 0.7 m^3 chamber and by 14 and 33 % in 56 m^3 chamber at 50 and 80 g/m^3 respectively. With initial MMADs and magnitude of particle growth observed in the present study, pulmonary (P) regional deposition would decrease. In the 0.7 m^3 chamber, P deposition would decrease by 17 and 16 % at the low and high loads, respectively. Decreases in P region fractional deposition would be greater in the 56 m^3 chamber, at 26 and 44 % for the low and high loads, respectively. Theoretical deposition fractions for given particle diameters are listed in **Table 4**. These large decreases in the P region would have greater significance for less soluble aerosols because of the relatively slower clearance from this compartment. However, because SFE particles are highly soluble, shifts in regional deposition pattern assume secondary relevance to TR deposition changes primarily because rapid dissolution of the particles decreases particle residence time in these regional compartments where, normally, other clearance mechanisms slower than particle dissolution would predominate.

System Atmosphere Differences and Potential Toxicity

An average (both load levels) relative aerosol dispersal efficiency ratio of $\cong 1.5$ for the 56 m^3 chamber conditions vs. the 0.7 m^3 conditions would favor a comparable 1.5 ratio for initial

aerosol deposition rate in lungs at a given minute ventilation (Ve). For example, at the 80 g/m^3 load level, an individual with a typical resting Ve of 7 L/min.[13] exposed to the 56 m^3 chamber atmosphere, at peak aerosol concentration of 14.0 g/m^3, would have 9.8 x 10^{-2} grams/min total lung deposition rate. This assumes an average (mean of all SFE MMADs) TR deposition fraction of 0.9, growth effects not withstanding (see **Table 4**). The same individual exposed to the 0.7 m^3 chamber atmosphere, at peak aerosol concentration of 10.0 g/m^3 , would have 7.0 x 10^{-2} g/min total lung deposition rate. At the 50 g/m^3 load, the corresponding deposition rates would be 7.1 x 10^{-2} g/min and 4.4 x 10^{-2} g/min.

Change in the percent baseline carboxyhemoglobin (COHb) level in man caused by breathing CO can be predicted by the following empirical equation[14].

$$\Delta\,[\text{COHb}]\% = (\text{CO} \times \text{Ve} \times t)/\,2.5 \times 10^4, \qquad [1]$$

where Ve is L/min., t is min., and CO is ppm. This algorithm was found applicable for humans breathing CO concentrations from 90 to 21,000 ppm for periods of 20 to 300 min. but with limited reliability at COHb concentrations above 80 %. As a point of reference, baseline COHb in non-smokers is 1.3 % and in smokers may vary from 5 to 10 %. Thus at a baseline Ve = 7 L/min. and exposure to the 50 and 80 g/m^3 (0.7 m^3 chamber) atmospheres for 20 min. the predicted COHb levels would be $\cong$ 14.4 and 37.4% . In the 56 m^3 chamber, corresponding COHb levels would be 30.7 and 56.8% at extrapolated initial CO concentrations.

These aerosol deposition and COHb formation calculations are based on the assumption of steady-state, peak concentrations of the constituents in the respective atmospheres and a fixed Ve. Because of the differing rates of change of the aerosol and gaseous component concentrations assessment and comparison of the potential toxicity of these atmospheres is much more complex than indicated. Assessment and comparison of the potential toxicity of these atmospheres is further complicated by the relative magnitude physiological responses that they elicit, for example, CO_2 induced hypercapnea and how this in turn effects the inhalation of other constituents of the atmosphere.

Respiratory sensitivity to CO_2 inhalation has long been recognized with respect to both stimulation of ventilation at low concentrations of CO_2 and to CO_2 induced narcosis, apnea,

and death at high concentrations. However the correlation between atmospheric CO_2 concentration and Ve is not linear and is more complicated than is superficially apparent. Early investigators demonstrated that the partial pressure of CO_2 (Pco_2) rather than fractional portion of CO_2 in respiratory gas was the determinant of the amount of gas in blood[15,16]. Haldane and Priestly[17] demonstrated the specific importance of the alveolar partial pressure of CO_2 ($PAco_2$) for regulation of breathing; showing that despite large changes in barometric pressure, $PAco_2$ remained relatively constant at approximately 40 mmHg. Carbon dioxide stimulation of respiration was demonstrated to be mediated by separate if not totally independent mechanisms than hypoxic stimulation of ventilation. Subsequently, research has lead to the current understanding of the importance of the CO_2 - H^+ - OCH_3^- system in regulation of breathing through action on peripheral (carotid body and aortic) and central (medullary) chemoreceptors[16]. Although atmospheric CO_2 concentration and $PAco_2$ are directly related, $PAco_2$ is greater than the corresponding atmospheric Pco_2 even when CO_2 enriched atmospheres are breathed. Despite the fact that the combined partial pressures of respiratory gases are generally lower than their atmospheric counterparts due to an increase in water vapor pressure in the lungs, the relative $PAco_2$ is elevated due numerous factors. Mixing of inspired gas with CO_2 enriched (from the previous breath) gas in the physiologic dead space, the exchange of CO_2 to the lung and O_2 to the blood serve to concentrate $PAco_2$. Consequently there are numerous other factors which influence $PAco_2$ including change in the relative fraction of dead space to tidal volume, the metabolic production of CO_2, the consumption of O_2, interaction with hypoxic stimulation of ventilation, work of ventilation, and respiratory exchange ratio or quotient ($R = \dot{V}CO_2/\dot{V}O_2$) to name a few. Exact quantitative descriptions based on well known physiological parameters, have been developed to describe various relationships in stable, steady-state gas exchange, normally on a breath by breath basis[18,19]. For example, $\Delta PAco_2$ can be calculated precisely if concentrations of inspired CO_2 and O_2, alveolar ventilation, and PAo_2 or ΔPAo_2 are either known or estimated with reasonable accuracy. These calculations, however, are not amenable for modification and use to describe the relationship between atmospheric CO_2 concentration and $PAco_2$ under other than steady-state conditions. Consequently, we have developed a series of first approximation and empirical quantitative expressions of the relationships between atmospheric CO_2 concentration, $PAco_2$ and Ve based on a review of the literature[16,18,20 through 35]. The purpose for the development of a dynamic, quantitative model of CO_2 induced hypercapnea was to describe

the effects of differing CO_2 concentrations and kinetics in the SFE atmospheres. A quantitative model of hypercapnea could then be used to model component interaction in the SFE atmospheres. Three dimentional graphs could then be developed to illustrate the relative impact of hypercapnea on aerosol particle depositon and carboxyhemoglobin formation from inhalation of CO. The 3-dimentional plots could then serve as a simple graphical method to compare the relative potential toxicity of these complex atmospheres.

Data reported in the literature relating Ve to P_{Aco_2} and atmospheric CO_2 concentration were fitted to the following regression with a coefficient of determination (r^2) of 0.991991 (**Figure 8**):

$$P_{Aco_2} = 33.8991 + 0.001493\ x^{0.9245} \qquad [2]$$

where, x = CO_2 (ppm),

33.8991≅ normal P_{Aco_2} (mmHg) not corrected to body temperature and pressure saturated (ie. 40 x 0.863 = 34.52) - see 19),

0.0014933 ≅ 0.00152 which is 2 times the conversion factor CO_2 ppm to mmHg (0.00076), the factor of 2 is required to account for partial pressure equilibrium between the alveolar space and blood assuming no metabolic CO_2 production; and

0.9245 ≅ the correction factor for barometric pressure sans water vapor pressure at 37 ° C. (ie. (760-713)/760 = 0.9382).

Non-linear regression analysis was applied to data from the literature relating P_{Aco_2} to Ve (**Figure 9**) resulting in the following empirical equation for a sigmoidal curve (r^2 = 0.99283):

$$Ve = 0.21387 + 62.2898/(1+\exp(-(x - 40.7476)/8.5355)) \qquad [3]$$

where, x = P_{Aco_2} (mmHg).

Equation 2 and equation 3 were combined and with additional data from the literature directly correlating CO_2 concentration and Ve were subject to a second non-linear regression analysis (r^2 = 0.99892) yielding the following empirical sigmoidal curve equation (**Figure 10**):

$$Ve = - 0.72562 + 63.9715/(1+\exp(-(x - 58949.29)/14807.62)) \qquad [4]$$

where, x = CO_2 (ppm).

The sigmoidal shape of the curves relating P_{ACO_2} and CO_2 concentration to Ve were similar to those described by Comroe[21] who noted that initial stimulation of breathing by CO_2 was neither rapid nor great until P_{ACO_2} had been elevated by approximately 10 to 15 mmHg. Severinghaus and Larson reported similar findings[33]. This initial moderate simulation of ventilation by CO_2 can be attributed to the buffering effects of blood and extracellular fluids which tends to limit H^+ stimulation of central and peripheral ventilatory receptors. Once the buffering capacity is exceeded the ventilatory response to CO_2 is nearly linear and much greater. The upper asymptotic limit of the Ve - CO_2 response curve has been attributed to occupation of receptor sites, onset of apnea from CO_2 narcosis (elevation of P_{ACO_2} by $\cong$ 70 mmHg) , and mechanical factors such as the Hering - Breuer reflex response to lung distention[16,20,21,26,33].

Equation 4 then was combined with the equations (all $r^2 \geq 0.998$) describing the exponential decay of CO_2 concentration in the SFE atmospheres (**see Figure 6**) to obtain a series of curves describing CO_2 induced hypercapnea for each SFE atmosphere for the one hour test period, assuming a baseline Ve of 7 L/min. (**Figure 11**). These transformations then were used to plot the fractional increase in aerosol particle deposition over the course of one hour of each of the SFE atmospheres assuming a 1:1 correlation between ventilation and aerosol deposition and a baseline Ve of 7 L/min. (**Figure 12**). Equation 4 transforms were combined with the equations (all $r^2 \geq 0.998$) characterizing the exponential aerosol concentration decay (**see Figure 4**) to determine hypercapnea driven increase in aerosol deposition rate. Baseline values were determined by assuming a resting Ve of 7 L/min. and inhalation of the lowest measured aerosol concentration of all the SFE atmospheres, 0.7 mg/L, giving a baseline deposition rate of 4.9 mg/min. The Ve functions, the aerosol concentration decay equations and corresponding aerosol deposition rate change calculations were used to generate 3-dimensional plots (**Figures 13,14,15 and 16**). When plotted on an equivalent scale the relative areas of the surface maps correspond to the relative difference in hypercapnea stimulated increase in aerosol particle deposition between the various SFE atmospheres. Because the extent of the surfaces mapped in these plots represents the range of exposure and physiological response, comparison of the surface maps serves as an index of relative potential health risk associated with breathing these atmospheres. For a given human exposure, both Δ Ve and Δ mg/L (aerosol concentration) change with time. Therefore the changes in deposition rate are defined by a line (diagonal or quasi-diagonal) lying

in the surface map depicted in these figures. The area of the imaginary plane "below" this "response" line which is normal to the XY plane (ie. parallel to the Z axis) is proportional to the total aerosol deposition increase. Total aerosol deposition change would be calculated as the integral of this resonse line, the area of which is bounded by the imaginary plane. The surface map ("response map") shown in the figures, which is a matrix composed of corresponding XYZ coordinates, is, in turn, proportional (as a function of Δ Z, by virtue of a common XYZ coordinate set) to the imaginary plane area[36,37]. Consequently the surface map area is proportional to and representative of total change of aerosol deposition for the corresponding SFE atmosphere, given the hypercapneic Δ Ve assumptions.

A similar process was used to examine the differences of Δ COHb %/min. formation rate (**Figures 17, 18,19 and 20**) and cumulative COHb %/min production (**Figures 21,22,23, and 24**) for each SFE atmosphere using the equations (all $r^2 \geq 0.995$) for exponential decay of CO concentration (see **Figure 5**) and equation 1 above. Like the 3-dimentional aerosol deposition plots, the relative area of the surface maps illustrates the relative magnitude SFE atmosphere induced COHb formation and thus of the potential toxicity of the SFE atmospheres. Likewise they serve to illustrate influence of component interaction on potential toxicity. The direct health risk of exposure to CO_2 at study concentrations and durations and of CO_2 induced hypercapnea is marginal. In fact, CO_2 inhalation at concentrations found in the test atmospheres has been used clinically to stimulate ventilation in the course of treatment of some metabolic disorders and in the evaluation of some respiratory diseases. Under the present circumstances the influence of calculated CO_2 induced hypercapnea on the potential toxicity of other components of these atmospheres was found to be remarkable, as indicated by comparison of the surface maps.

The task of assessing and comparing the potential toxicity of complex, multi-component, multi-phasic atmospheres which also are dynamic with respect to concentration and interaction of the components presents challenge to toxicologists and other environmental health risk assessment professionals. Precise reproduction in the laboratory of complex atmospheres encountered in industrial and environmental settings, for toxicity evaluation, often is not possible due to restrictions of the laboratory setting. The need for extensive field characterization of potential hazards and the development new strategies for comparison of laboratory test atmospheres with "real-life" counterparts are essential to enhance the validity of toxicity and

safety evaluation studies. The present investigation provided an opportunity to employ one such approach by using a 3-dimentional graphical means to illustrate the relative potential toxicity of SFE atmospheres which at cursory observation are not readily apparent and for which the effects of constituent interaction are not obvious. The use of a 3-dimentional graphial approach to integrate the effects of well characterized (albeit calculated) physiological responses to the inhaled atmospheres provides an additional tool for examining the potential effects of component interaction in complex, multi-component atmospheres. In the present investigation an illustrative, graphical approach to data analysis in conjunction with more conventional techniques enhanced the application of laboratory inhalation toxicity study results to the assessment of the potential hazard of "real-life" atmospheres when the laboratory conditions do not permit exact recreation of those "real-life" atmospheres.

REFERENCES

1. RS Sheinson, HG Eaton, RG Zalosh, BH Black, R Brown, H Burchell, G Salmon and WD Smith. Fire Extinguishment by Fine Aerosol Generation. *Proceedings of CFC and Halon Alternatives Conference.* October 20-22, Washington, DC, (1993a).

2. RS Sheinson, HG Eaton, BH Black, R Brown, H Burchell, G Salmon, J. St. Aubin and WD Smith. Total Flooding Fire Suppressant in a 56 m^3 (2000 ft^3) Compartment. In: *Proceedings of the Halon Alternatives Technical Working Conference 1993.* May 11-13, Albuquerque, NM, (1993b).

3. RS Sheinson, HG Eaton, RG Zalosh, BH Black, R Brown, H Burchell, G Salmon and WD Smith. Intermediate Scale Fire Extinguishment by Pyrogenic Solid Aerosol. *Proceedings of Halon Options Technical Working Conference.* May 3 - 5, Albuquerque, NM, (1994).

4. EC Kimmel and KL Yerkes. Design, Performance and Fluid Mechanics of a Small Animal, Whole-body Inhalation Exposure Chamber. In: 1989 Toxic Hazards Research Unit Annual Report. Armstrong Aerospace Medical Research Laboratory, Wright-Patterson AFB, OH. *(AAMRL-TR-90-051),* (1990).

5. SJ Rothenberg, DK Flynn, AF Eidson, JA Mewhinney and GJ Newton. Determination of Specific Surface Area by ^{85}Kr Adsorption, Comparison of Three Different Methods of Determining Surface Area and Evaluation of Different Specific Surface Area Standards. *J. Colloid Interface Sci.* 116: 541-551, (1987).

6. EP Radford. The Physics of Gases. In: WO Fenn and H Rahn (Eds) *Handbook of Physiology Section 3: Respiration I.* The American Physiological Society, by Waverly Press, Inc. Baltimore, MD, (1964).

7. EC Kimmel, EA Smith, LE Bowen, JE Reboulet, SJ Rothenberg and RL Carpenter. Physical and Chemical Characterization of Aerosols of Three Formulations of SFE, a Potential Dry Powder Replacement for Ozone Depleting Fire Suppressants. Presented at *Halon Options Technical Working Conference,* May 4, Albuquerque, NM, (1994) .

8. WC Hinds. *Aerosol Technology: Properties, Behavior, and Measurement of Airborne Particles.* John Wiley & Sons, Inc. New York, NY, (1982).

9. EC Kimmel, EA Smith, JE Reboulet, BH Black, RS Sheinson and RL Carpenter. Physicochemical Characterization of SFE Fire Suppressant Atmospheres: Comparison of Small

with Large Scale Laboratory Atmospheres. In: *Proceedings of Halon Options Technical Working Conference 1995.* May 9-11. Albuquerque, NM, (1995).

10. SK Friedlander. *Smoke, Dust and Haze: Fundamentals of Aerosol Behavior.* John Wiley and Sons. Inc. New York, NY, (1977).

11. OG Raabe. Experimental Dosimetry: Introduction. In *Extrapolation of Dosimetric Relationships for Inhaled Particles and Gases.* Eds. JC Crapo, ED Smolko, FJ Miller, JA Graham and AW Hayes. Academic Press, Inc. San Diego, CA, (1989).

12. Y-S Cheng and H-C Yeh. A Model for Aerosol Deposition in the Human Tracheobronchial Region. *Am. Ind. Hyg. Assoc. J.* 42: 771-776, (1981).

13. RD Dripps and JH Comroe Jr. The Respiratory and Circulatory Response of Normal Man to Inhalation of 7.6 and 10.4 % CO_2 with a Comparison of the Maximal Ventilation Produced by Severe Muscular Exercise, Inhalation of CO_2 and Maximal Voluntary Hyperventilation. *Am. J. Physiol.* 149: 43-51, (1947) .

14. N Pace, E Strajman and EL Walker. Acceleration of Carbon Monoxide Elimination in Man by High Pressure Oxygen. *Science* 111: 652-654, (1979).

15. J Setschenow. Sur Frage uberDie Athmungi Verdunnter Luft. *Arch Ges. Physiol.* 22: 252-261, (1880).

16. RH Kellogg. Central Chemical Regulation of Respiration. In: WO Fenn and H Rahn (Eds) *Handbook of Physiology Section 3: Respiration I.* The American Physiological Society, by Waverly Press, Inc. Baltimore, MD, (1964).

17. JS Haldane, and JG Priestly. The Regulation of the Lung-Ventilation. *J. Physiol., London.* 32: 225-266, (1905).

18. JW Bellville and JC Seed. Respiratory Carbon Dioxide Response Curve Computer. *Science* 130:1079-1084, (1959) .

19. AB Otis. Quantitative Relationships in Steady-state Gas Exchange. In: WO Fenn and H Rahn (Eds) *Handbook of Physiology Section 3: Respiration I.* The American Physiological Society, by Waverly Press, Inc. Baltimore, MD, (1964).

20. RM Cherniak. Work of Breathing and the Ventilatory Response to CO_2. In: WO Fenn and H Rahn (Eds) *Handbook of Physiology Section 3: Respiration II.* The American Physiological Society, by Waverly Press, Inc. Baltimore MD, (1964) .

21. JH Comroe *Physiology of Respiration: An Introductory Text.*, Year Book Medical Publishers, Inc. Chicago, IL, (1974).

22. DJC Cunningham, DG Shaw, S Lahiri and BB Lloyd. The Effect of Maintained Ammonium Chloride Acidosis on the Relation Between Pulmonary Ventilation and Alveolar Oxygen and Carbon Dioxide in Man. *Quart. J. Exptl. Physiol.* 46: 323-334, (1961).

23. JE Eckenhoff, M Helrich and MJD Hege. Effect of Narcotics, Thiopental and Nitrous Oxide upon Respiration and Respiratory Response to Hypercapnea. *Anesthesiology,* 19: 240-253, (1985).

24. JG Gabbard, A Roos, DE Eastwood and TH Burford. Effect of Ether Anesthesia upon Alveolar VEntilation and Acid-base Balance in Man. *Ann. Surg.* 136: 680-686, (1952).

25. CJ Lambertsen. Carbon dioxide and Respiration in Acid-base Homeostasis. *Anesthesiology,* 21: 642-656, (1960).

26. CJ Lambertsen. Effects of Drugs and Hormones on the Respiratory Response to Carbon Dioxide. In: WO Fenn and H Rahn (Eds) *Handbook of Physiology Section 3: Respiration I.* The American Physiological Society, by Waverly Press, Inc. Baltimore, MD, (1964).

27. CM Landmesser, S Cobb, AS Peck, and JG Converse. Respiratory Responses to Carbon Dioxide "Transients" in Normal Volunteers. *Anesthesiology,* 58: 807-830, (1975).

28. BB Lloyd, MGM Jukes and DJC Cunningham. The Relationship Between Alveolar Oxygen Pressure and The Respiratory Response to Carbon Dioxide in Man. *Quart. J. Exptl. Physiol.* 43: 214-227, (1958).

29. HH Loeschcke, A Sweel, RH Kough and CJ Lambertsen. The Effect of Morphine and Of Mepiridine upon the Respiratory Response of Normal Men to Low Concentrations of Inspired Carbon Monoxide. *J. Pharmacol. Exptl. Therap.* 108: 376-383, (1953).

30. M Nielsen and H Smith. Studies on the Regulation of Respiration in Acute Hypoxia. With an Appendix on Respiratory Control During Prolonged Hypoxia. *Acta Physiol. Scand.* 24: 293-131, (1952).

31. C Papadopaulos and AS Keats. Specific and Non-specific Antagonism of Morphine Induced Respiratory Depression. *Anesthesiology,* 23: 86-91, (1962) .

32. DJ Reed and RH Kellogg. Changes in Respiratory Response to CO_2 During Sleep and at Sea Level and at Altitude. *J. Appl. Physiol.* 13: 325-330, (1985).

33. JW Sveringhaus and CP Larson Jr. Respiration in Anesthesia. In: WO Fenn and H Rahn (Eds) *Handbook of Physiology Section 3: Respiration II.* The American Physiological Society, by Waverly Press, Inc. Baltimore, MD, (1964).

34. SM Tenney. The Interpretation of Respiratory Drug Effects in Man. *Anesthesiology*, 17: 82-93, (1956).

35. USHEW -U.S. Department of Health, Education and Welfare. *Criteria for a Recommended Standard...Occupational Exposure to Carbon Dioxide.* Public Health Service, Center for Disease Control, National Institute for Occupational Safety and Health, HEW # (NIOSH) 76-194, (1976).

36. CE Pearson. *Handbook of Applied Mathematics: Selected Results and Methods.* Van Norstrand Reinhold Co., Inc. New York, NY, (1983).

37. M Abramowitz and IA Segun. *Handbook of Mathematical Functions with Formulas, Graphs, and Mathematical Tables.* National Bureau of Standards, Applied Mathematics Series # 35, U.S. Government Printing Office, Washington, DC, (1964).

TABLE 1.
EXPERIMENTAL DESIGN
ATMOSPHERE CHARACTERIZATION

Chamber	Target Concentration	Number of Trials
0.7 m^3	50 g/m^3	3
0.7 m^3	80 g/m^3	4
56 m^3	50 g/m^3	3
56 m^3	80 g/m^3	2

TABLE 2. AEROSOL SPATIAL DISTRIBUTION - 56 m^3 CHAMBER

Height from floor	Concentration g/m^3		Size	MMAD - µm
	1.5 min.	60 min.	1.5 min	60 min
0.3 m	10.1	1.8	2.9	5.2
1.0 m	10.9	1.9	3	4.9
1.75 m	10.9	1.9	2.9	4.4
3.3m	11.4	2	3	5.1

TABLE 3. CO_2 SPATIAL DISTRIBUTION - 56 m^3 CHAMBER

Height from floor	Concentration g/m^3			
	1.5 min.	2.5 min.	30 min.	60 min.
0.3 m	23.4	24.2	-	11.2
1.0 m	26.5	25.4	17	13.9
1.75 m	26.2	26.7	18.2	12.2
3.3 m	26.4	24.9	-	11.2

TABLE 4.
AEROSOL GROWTH EFFECT ON PARTICLE DEPOSITION

EXP.	SIZE		DEPOSITION FRACTION							
	initial	*max.*	T R		N P		T B		P	
	(μm)	*(μm)*	*initial*	*max.*	*initial*	*max.*	*initial*	*max.*	*initial*	*min.*
0.7 - 50	2.8	3.8	0.87	0.93	0.06	0.23	0.06	0.13	0.63	0.46
0.7 - 80	3	4	0.9	0.94	0.12	0.24	0.08	0.16	0.59	0.44
56 - 50	2.8	3.8	0.87	0.95	0.08	0.33	0.07	0.21	0.63	0.37
56 - 80	2.4	6.3	0.78	0.97	0	0.45	0.05	0.37	0.66	0.23

TR = total respiratory system, NP = nasopharyngeal region ,TB = tracheobronchial region, P = pulmonary (alveolar) region ,0.7 - 50 = 0.7 m^3 chamber at 50 g/m^3, 0.7 - 80 = 0.7 m^3 chamber at 80 g/m^3 , 56 - 50 = 56 m^3 chamber at 50 g/m^3, 56 - 80 = 56 m^3 chamber at 80 g/m^3.

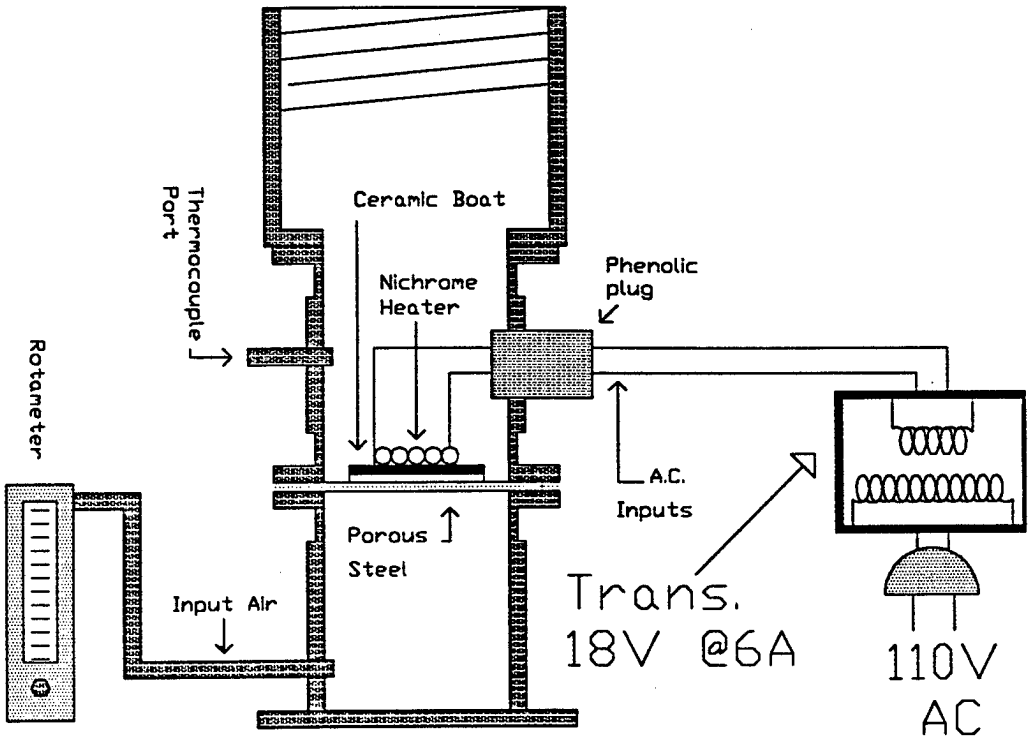

Figure 1. Cross-section of the SFE aerosol generator - 0.7 m^3 chamber.

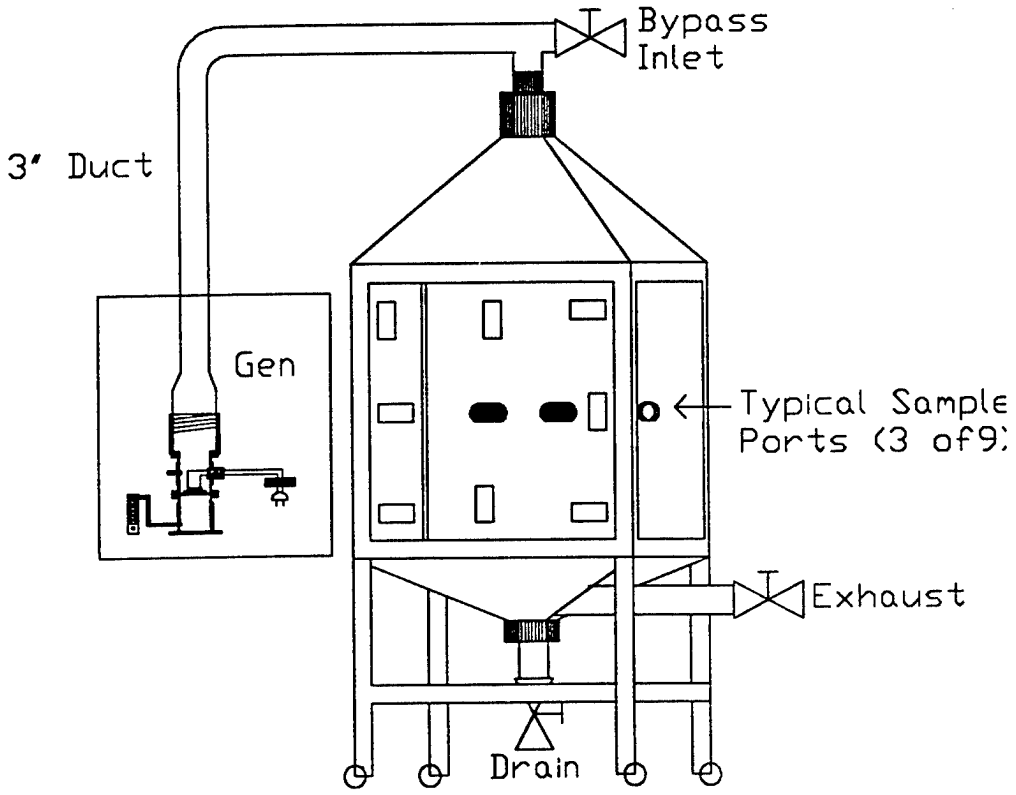

Figure 2. Diagram of the 0.7 m^3 chamber inhalation exposure system

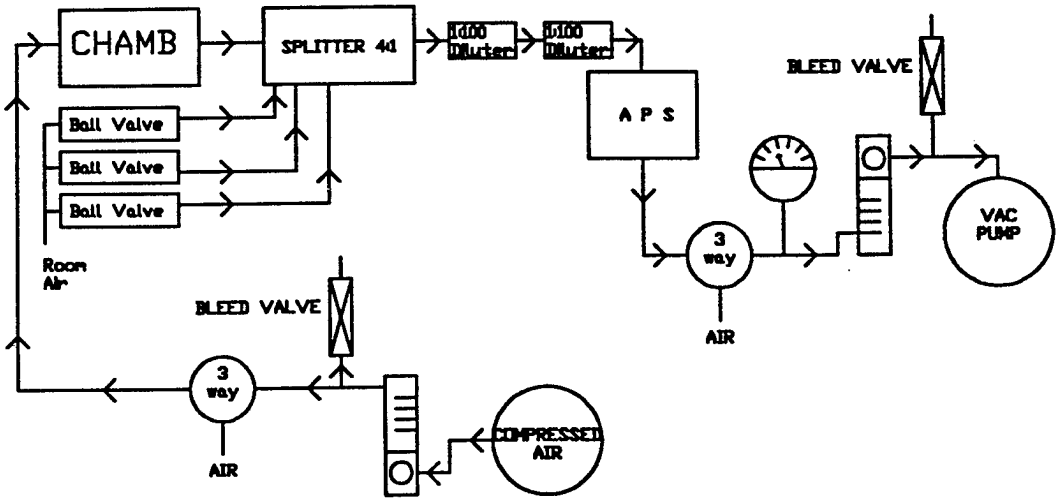

Figure 3. Schematic of the aerosol sampling dilution system.

*** 3-way solenoid valves switched simultaneously, flow meters balanced to maintain zero differential chamber pressure**

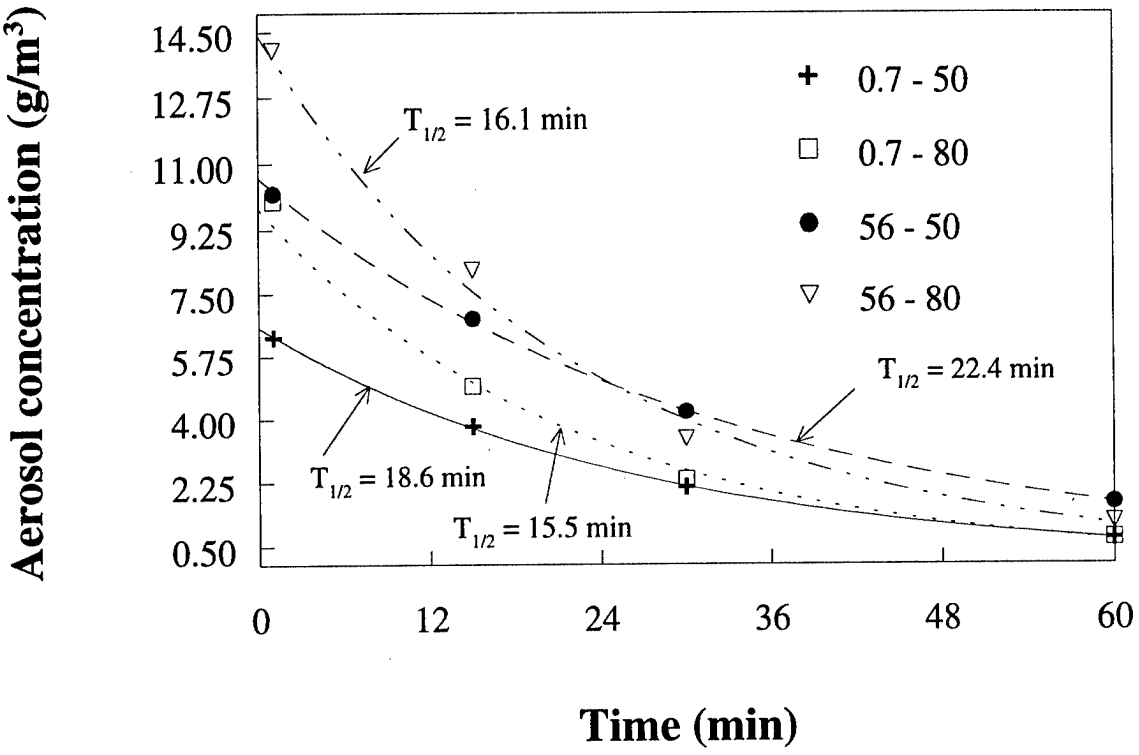

Figure 4. Exponential decay of actual aerosol concentration.

0.7 - 50 = 0.7 m^3 chamber at 50 g/m^3
0.7 - 80 = 0.7 m^3 chamber at 80 g/m^3
56 - 50 = 56 m^3 chamber at 50 g/m^3
56 - 80 = 56 m^3 chamber at 80 g/m^3

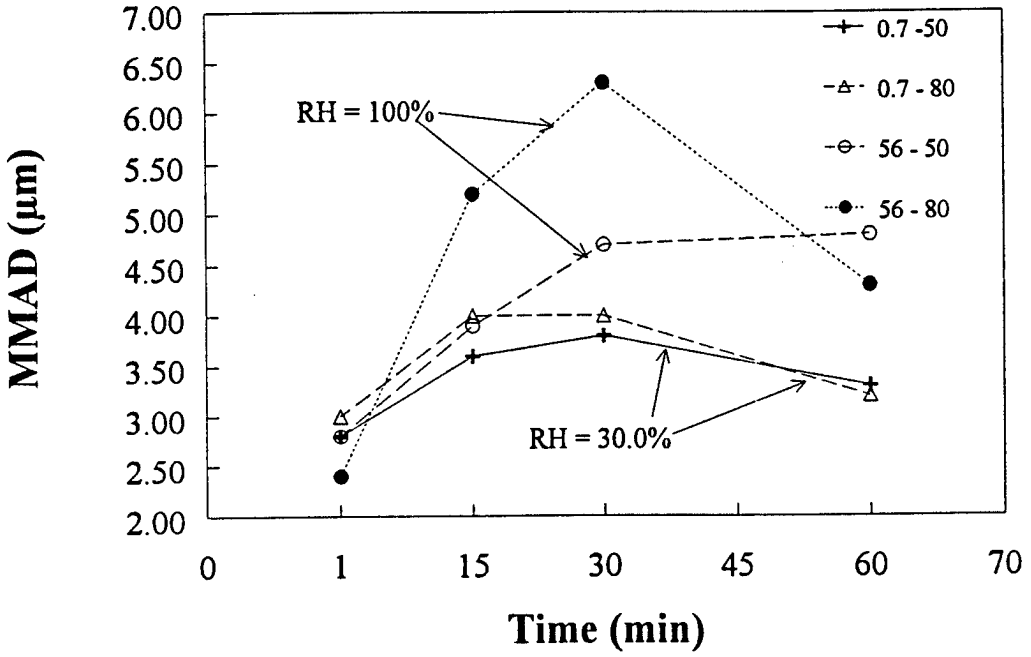

Figure 5. Aerosol particle growth

0.7 - 50 = 0.7 m³ chamber at 50 g/m³
0.7 - 80 = 0.7 m³ chamber at 80 g/m³
56 - 50 = 56 m³ chamber at 50 g/m³
56 - 80 = 56 m³ chamber at 80 g/m³

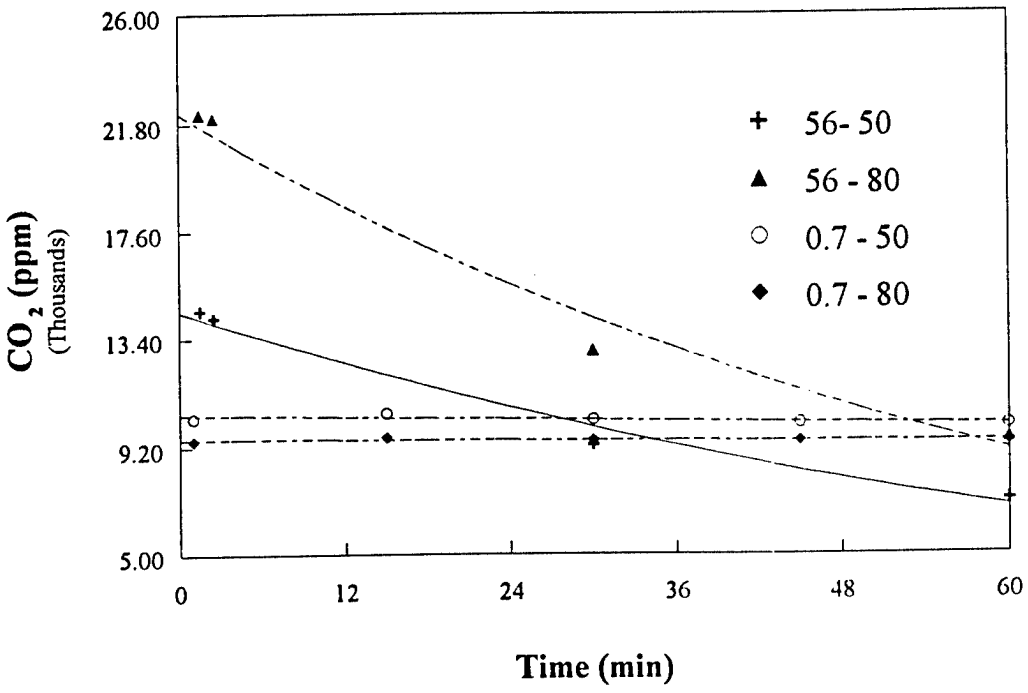

Figure 6. Exponential decay of CO_2 concentration.

0.7 - 50 = 0.7 m^3 chamber at 50 g/m^3
0.7 - 80 = 0.7 m^3 chamber at 80 g/m^3
56 - 50 = 56 m^3 chamber at 50 g/m^3
56 - 80 = 56 m^3 chamber at 80 g/m^3

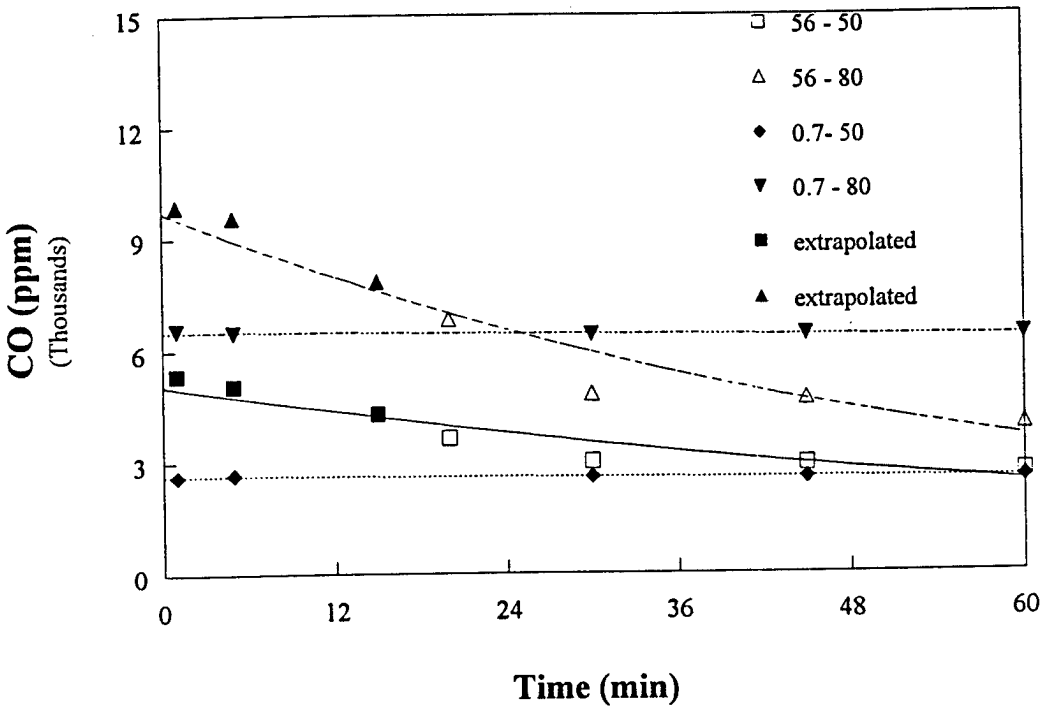

Figure 7. Exponential decay of CO concentration.

0.7 - 50 = 0.7 m^3 chamber at 50 g/m^3
0.7 - 80 = 0.7 m^3 chamber at 80 g/m^3
56 - 50 = 56 m^3 chamber at 50 g/m^3
56 - 80 = 56 m^3 chamber at 80 g/m^3

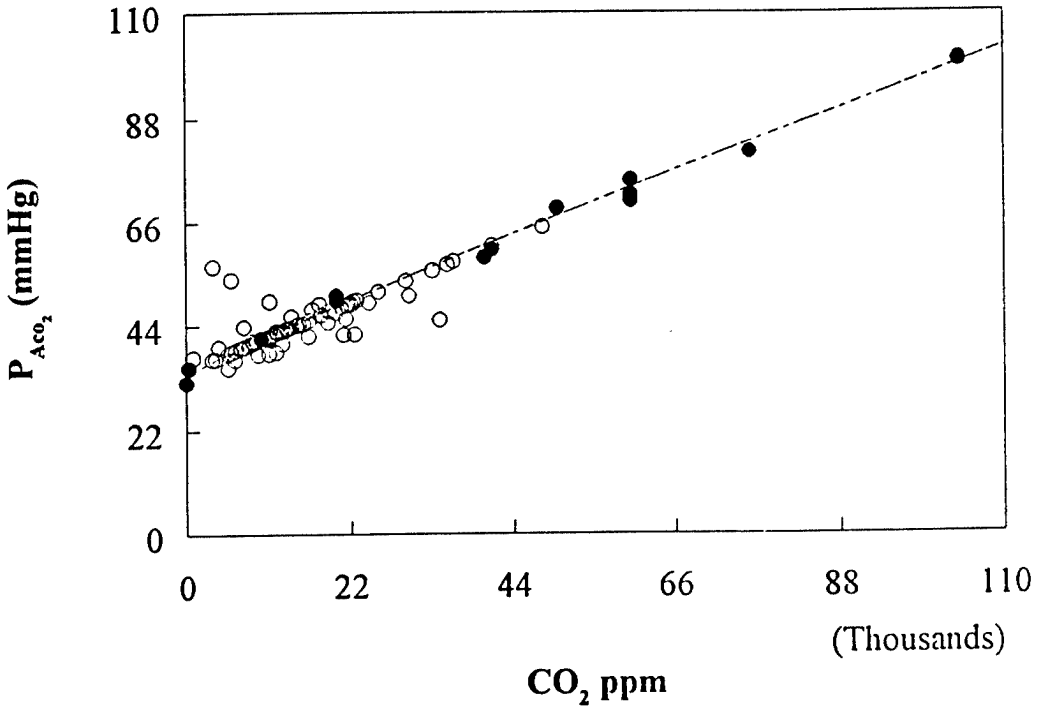

Figure 8. Alveolar CO_2 partial pressure as a function of atmospheric CO_2 concentration.
solid circles = CO_2 concentration and P_{Aco_2} reported directly
open circles = CO_2 concentration reported and P_{Aco_2} reported as diffential from baseline

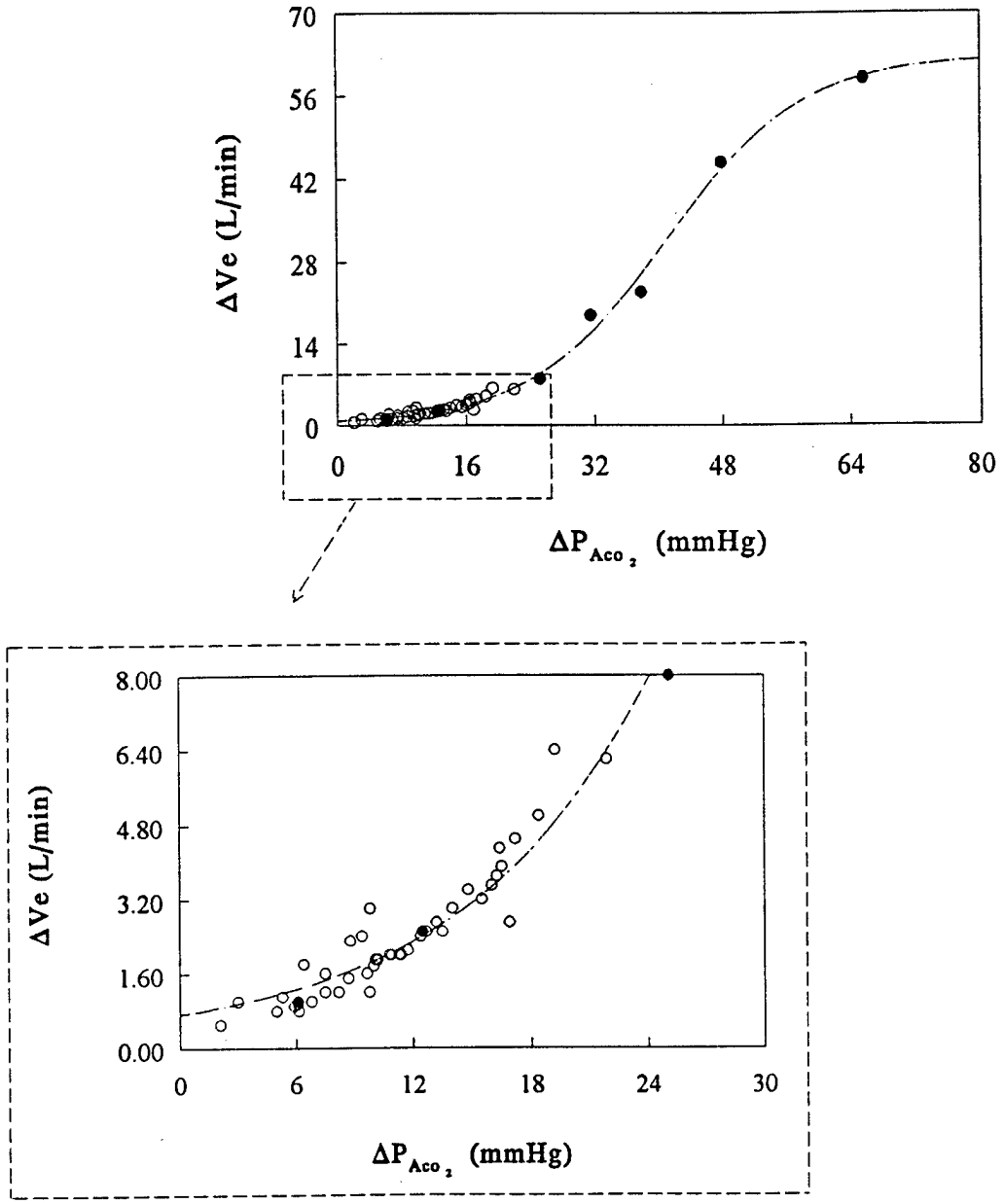

Figure 9. Elevation of minute ventilation due to hypercapnea as a function of alveolar CO_2 partial pressure.

solid circles = Ve, CO_2 concentration and P_{Aco_2}

open circles = Ve, P_{Aco_2} given and CO2 concentration calculated

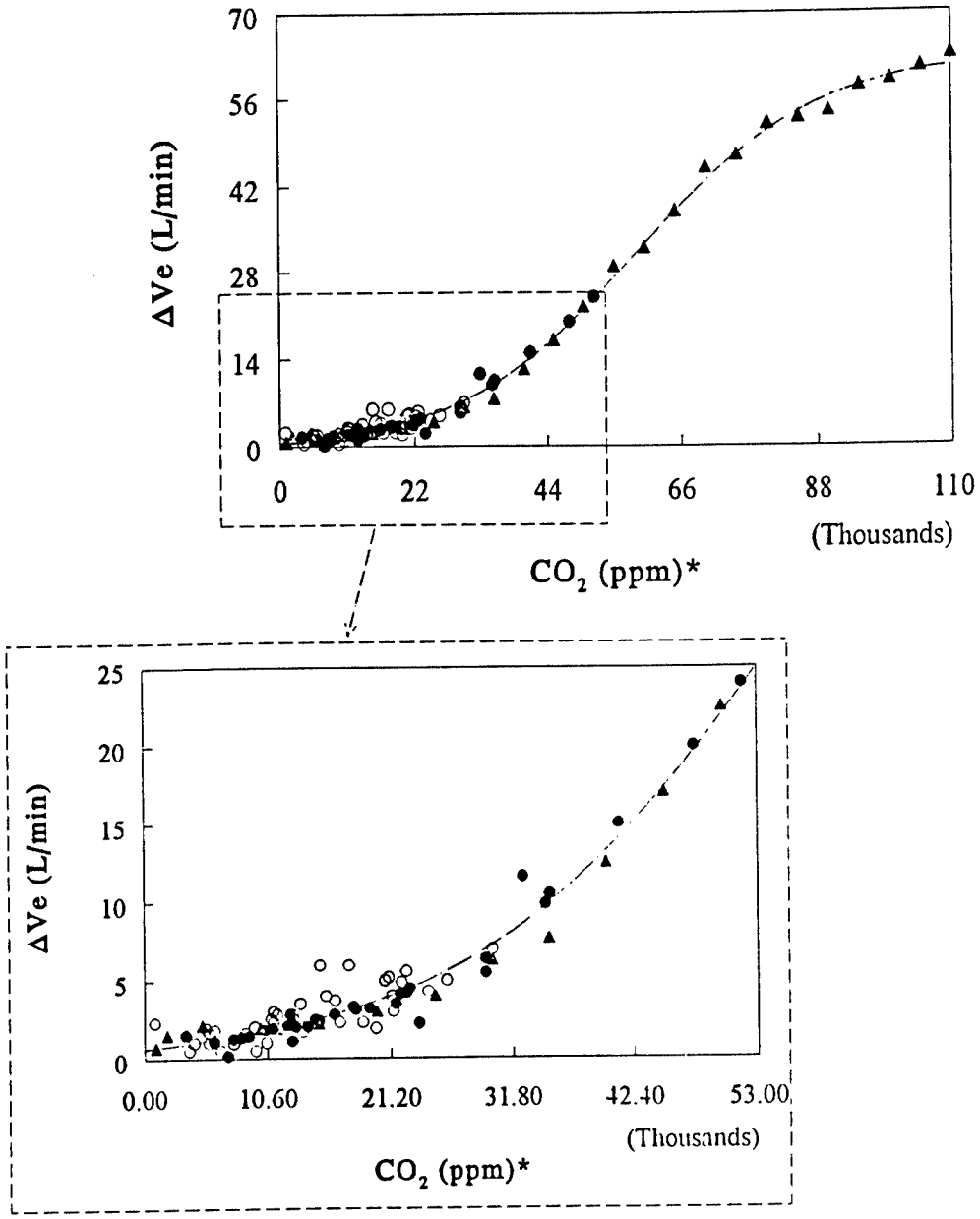

Figure 10. Elevation of minute ventilation due to hypercapnea as a function of atmospheric CO_2 concentration.

*** based on $PAco_2$ calculations, solid circles = Ve, CO_2 concentration and $PAco_2$ given open circles = Ve, $PAco_2$ given and CO_2 concentration calculated triangles = data reported as CO_2 vs Ve directly**

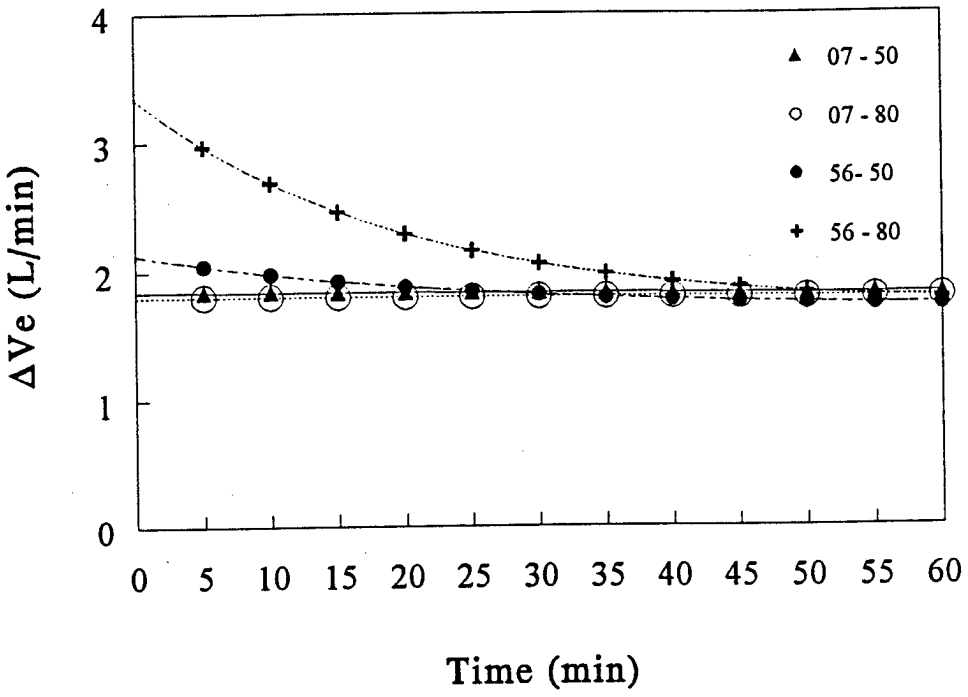

Figure 11. Hypothetical CO_2 induced hypercapnea for each exposure condition.

0.7 - 50 = 0.7 m^3 chamber at 50 g/m^3
0.7 - 80 = 0.7 m^3 chamber at 80 g/m^3
56 - 50 = 56 m^3 chamber at 50 g/m^3
56 - 80 = 56 m^3 chamber at 80 g/m^3

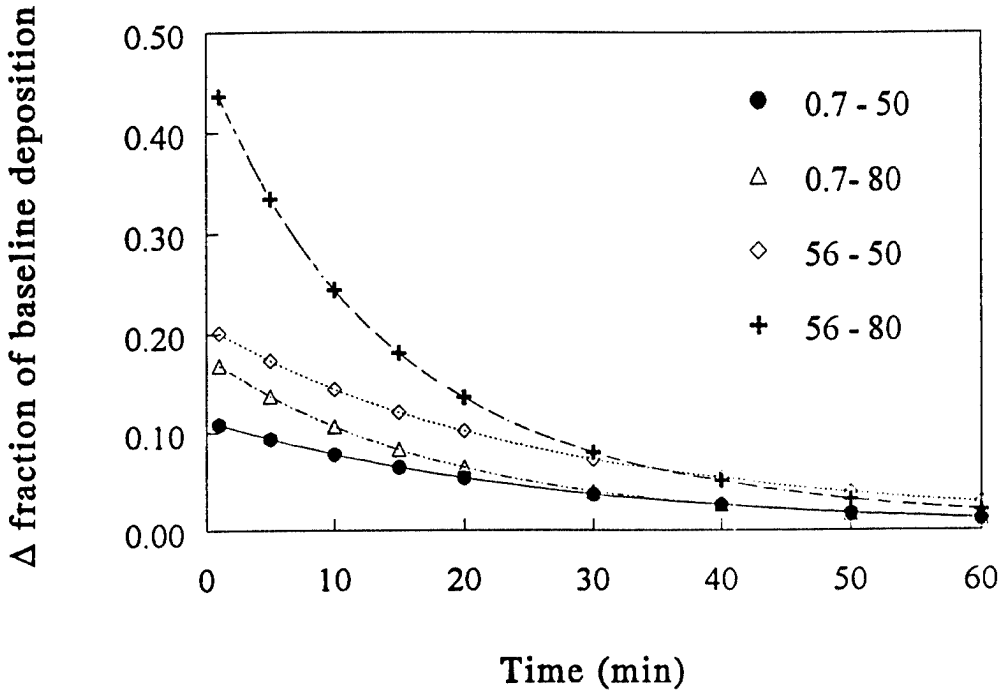

Figure 12. Calculated fractional increase of aerosol depositon due to CO_2 induced hypercapnea

assumes direct proportionality between deposition and Ve
Ve = 7 L/min = baseline
0.7 - 50 = 0.7 m^3 chamber at 50 g/m^3
0.7 - 80 = 0.7 m^3 chamber at 80 g/m^3
56 - 50 = 56 m^3 chamber at 50 g/m^3
56 - 80 = 56 m^3 chamber at 80 g/m^3

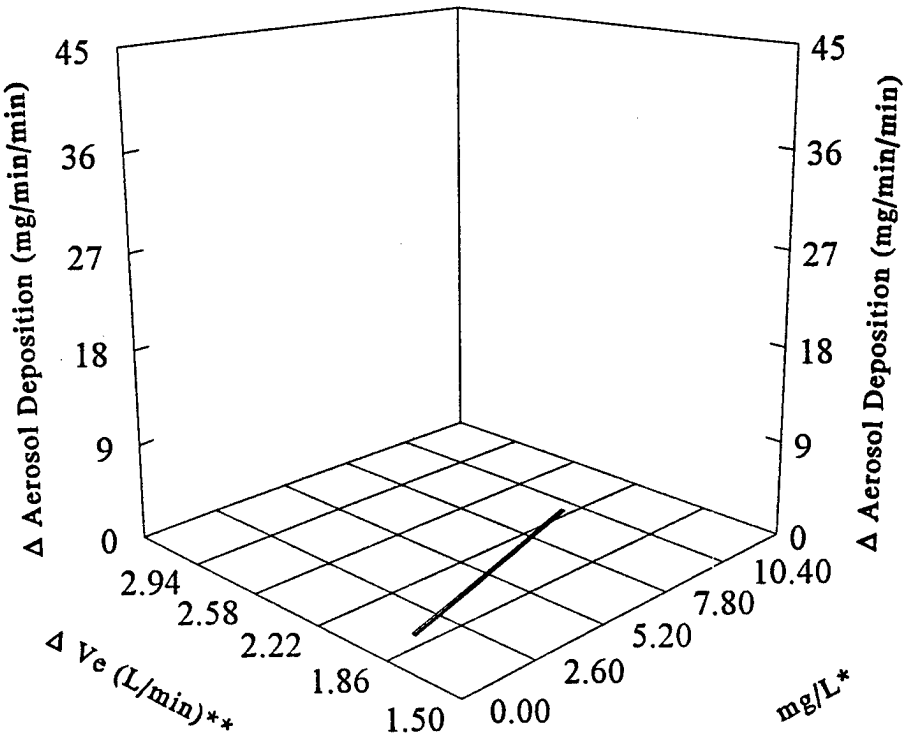

Figure 13. Increase in particle deposition as a function of aerosol mass concentration and CO_2 induced hypercapnea - 0.7 m^3 chamber at 50 g/m^3.

*** greater than baseline concentration of 0.7 mg/L (lowest encountered in all 4 atmospheres)**

**** greater than baseline Ve of 7 L/min.**

Under these conditions, little variation of aerosol deposition rate is predicted.

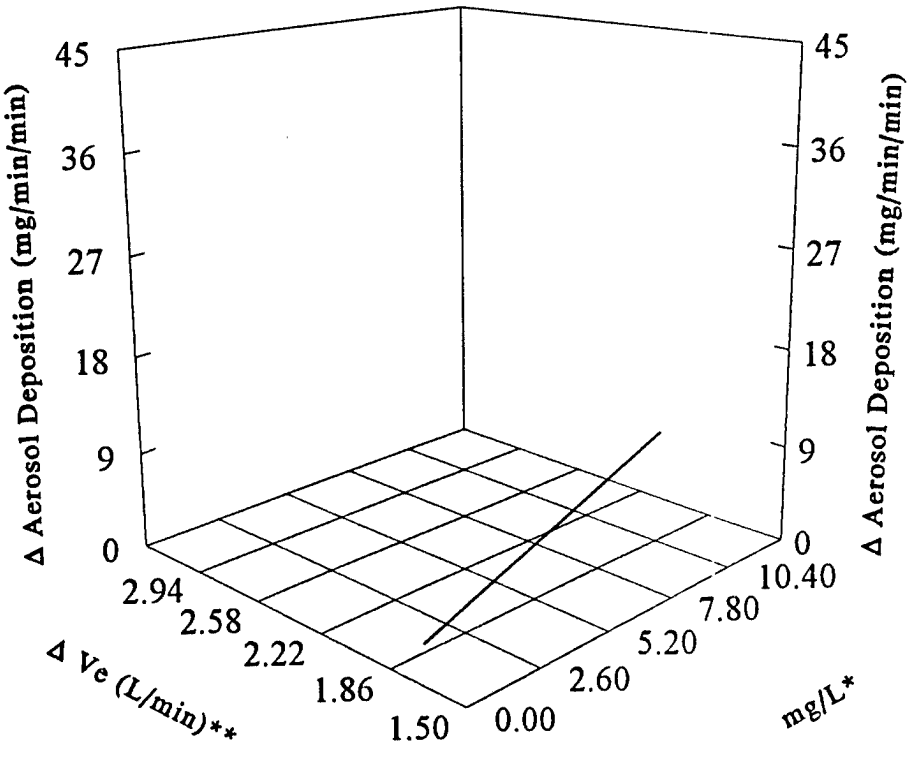

Figure 14. Increase in particle deposition as a function of aerosol mass concentration and CO_2 induced hypercapnea - 0.7 m^3 chamber at 80 g/m^3.

*** greater than baseline concentration of 0.7 mg/L (lowest encountered in all 4 atmospheres)**

**** greater than baseline Ve of 7 L/min.**

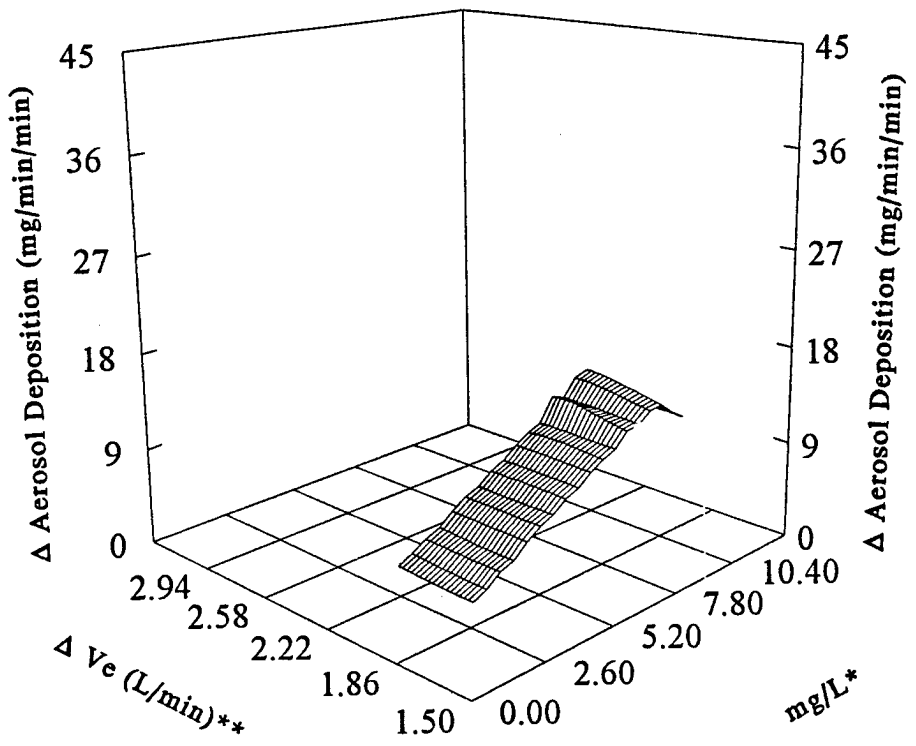

Figure 15. Increase in particle deposition as a function of aerosol mass concentration and CO_2 induced hypercapnea - 56 m^3 chamber at 50 g/m^3.

*** greater than baseline concentration of 0.7 mg/L (lowest encountered in all 4 atmospheres)**

**** greater than baseline Ve of 7 L/min.**

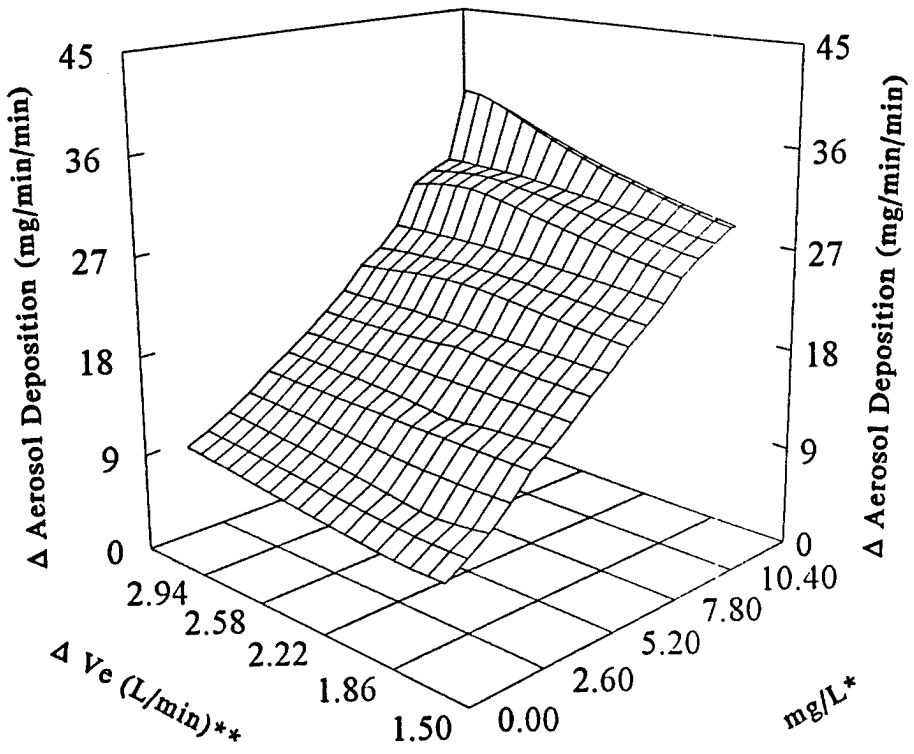

Figure 16. Increase in particle deposition as a function of aerosol mass concentration and CO_2 induced hypercapnea - 56 m^3 chamber at 80 g/m^3.

*** greater than baseline concentration of 0.7 mg/L (lowest encountered in all 4 atmospheres)**

**** greater than baseline Ve of 7 L/min.**

Under these exposure conditions, a much larger change of aerosol deposition rates is anticipated.

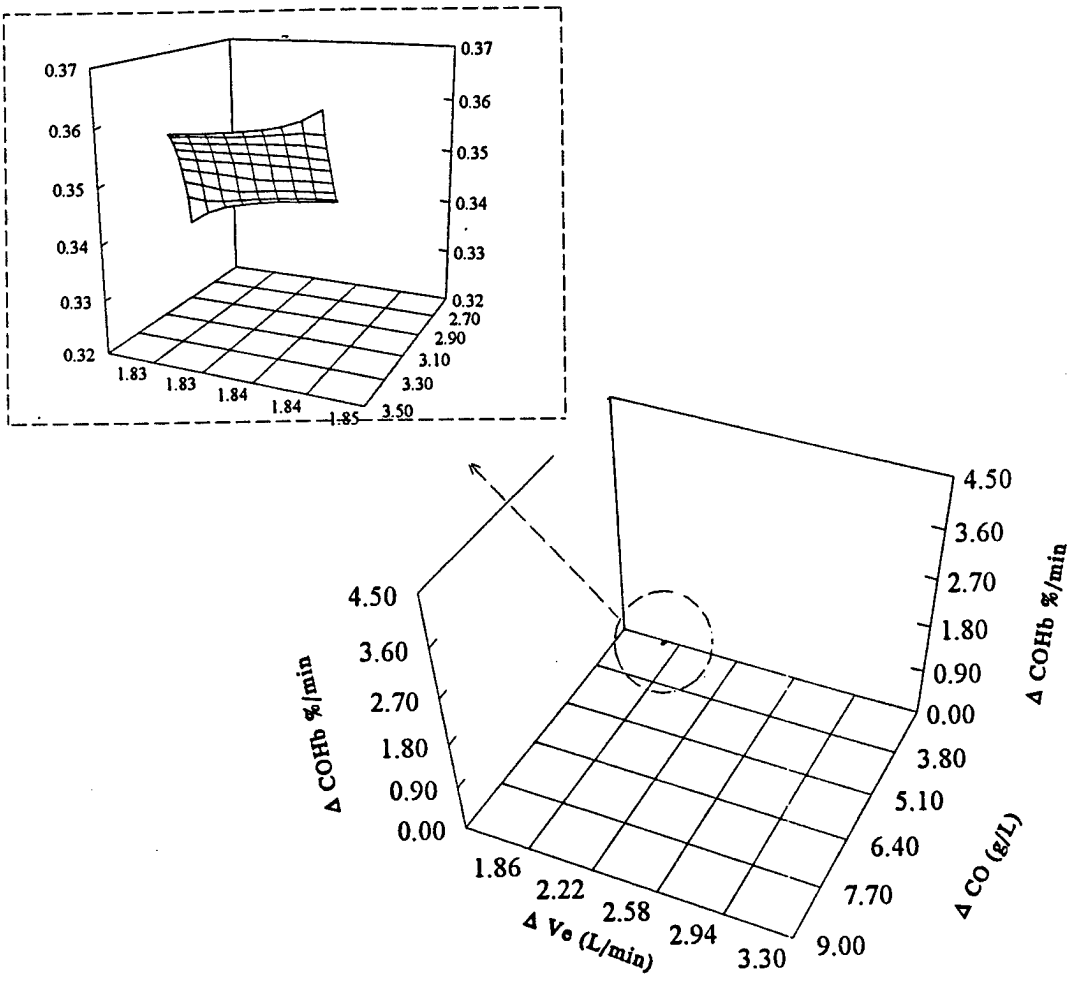

Figure 17. Change of carboxyhemaglobin formation rates - 0.7 m^3 chamber at 50 g/m^3.

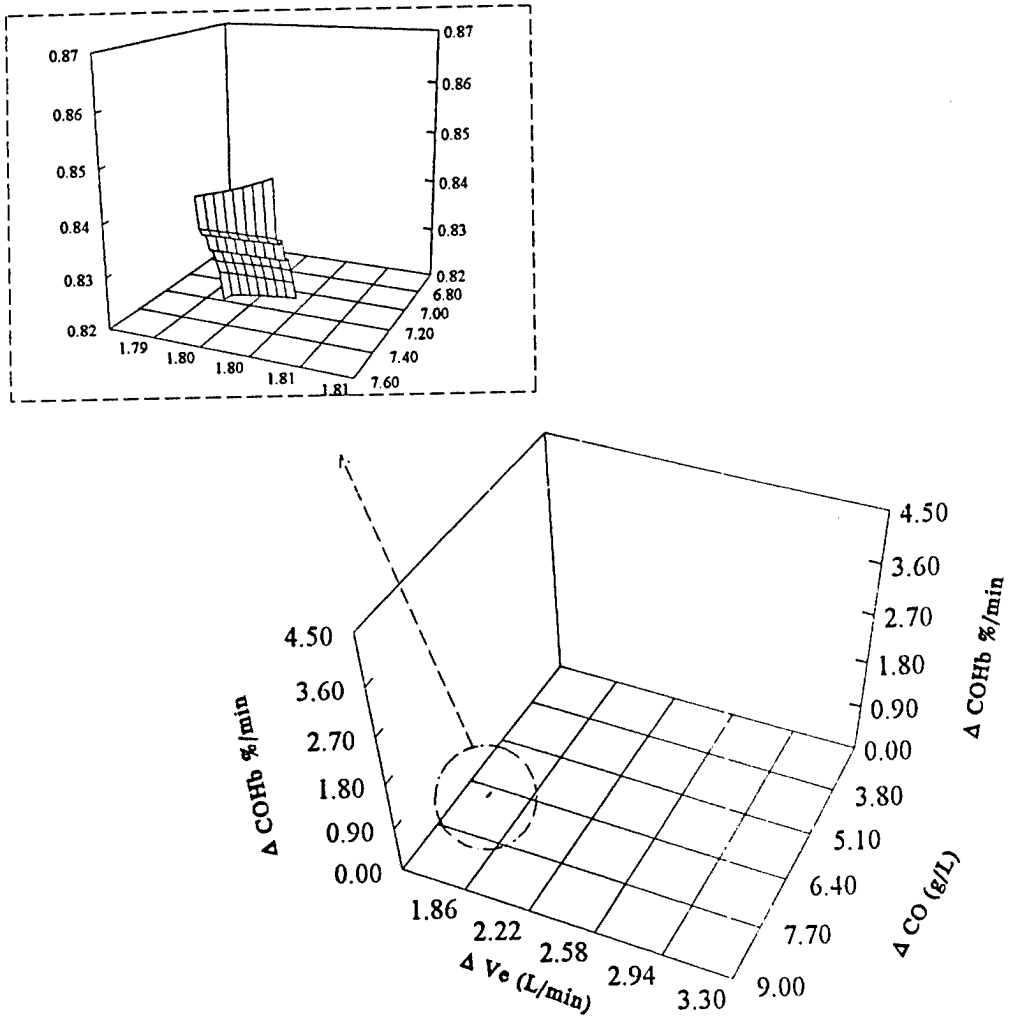

Figure 18. Change of carboxyhemoglobin formation rates - 0.7 m^3 chamber at 80 g/m^3.

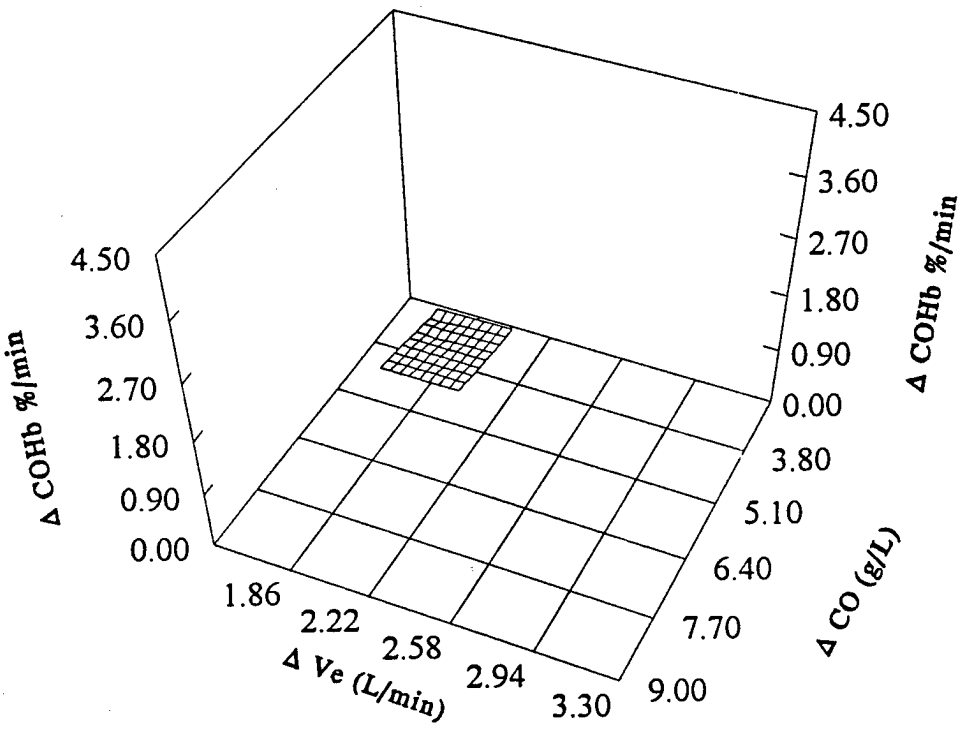

Figure 19. Change of carboxyhemoglobin formation rates - 56 m^3 chamber at 50 g/m^3.

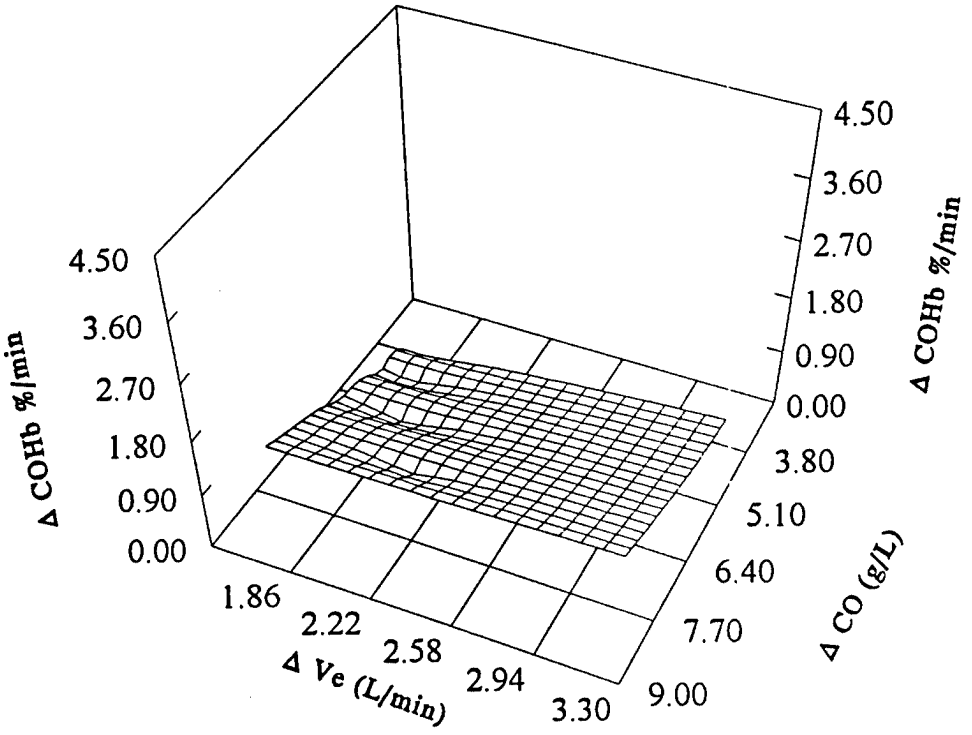

Figure 20. Change of carboxyhemoglobin formation rates - 56 m^3 chamber at 80 g/m^3.

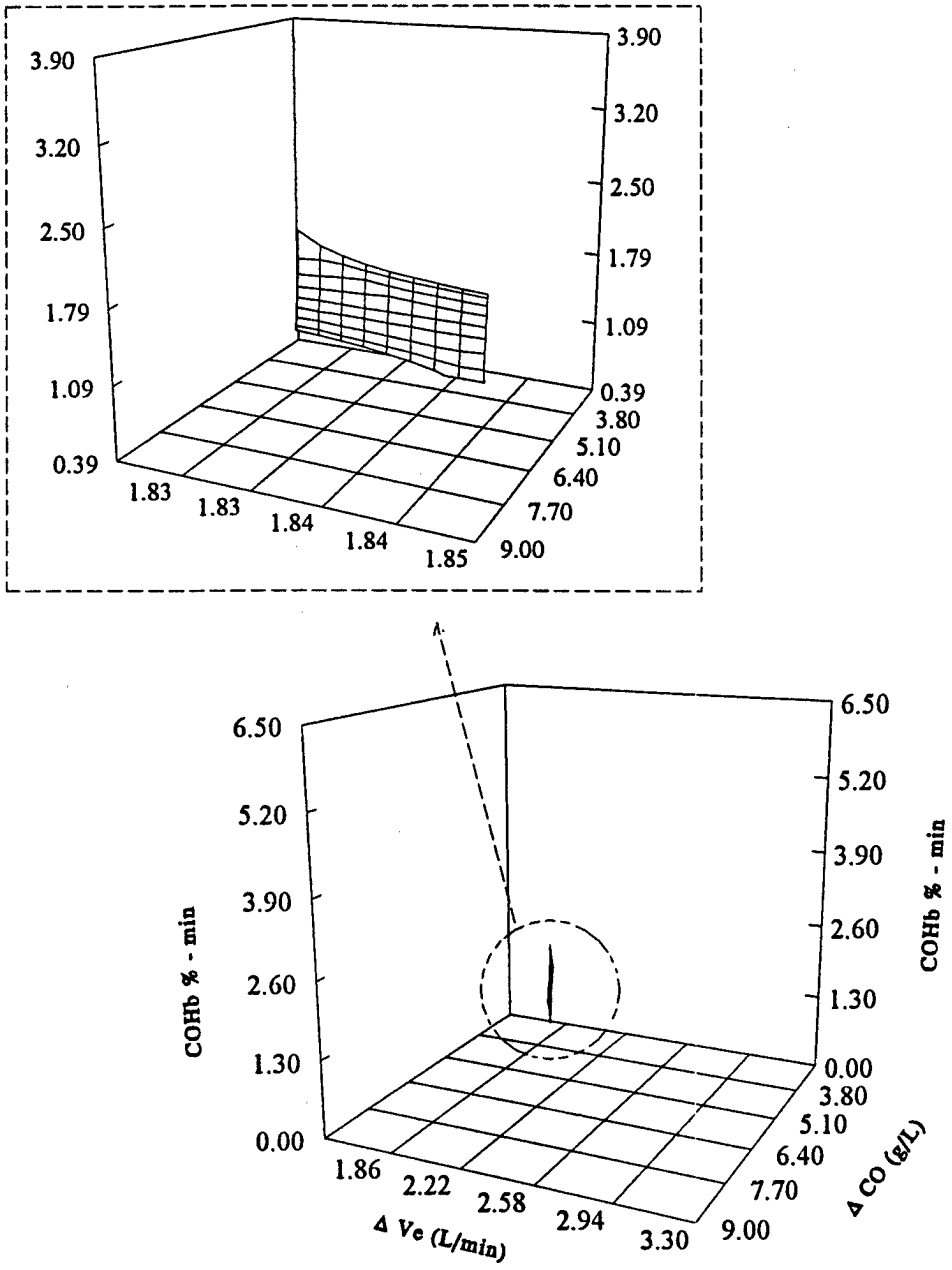

Figure 21. Cumulative carboxyhemoglobin formation - 0.7 m^3 chamber at 50 g/m^3.

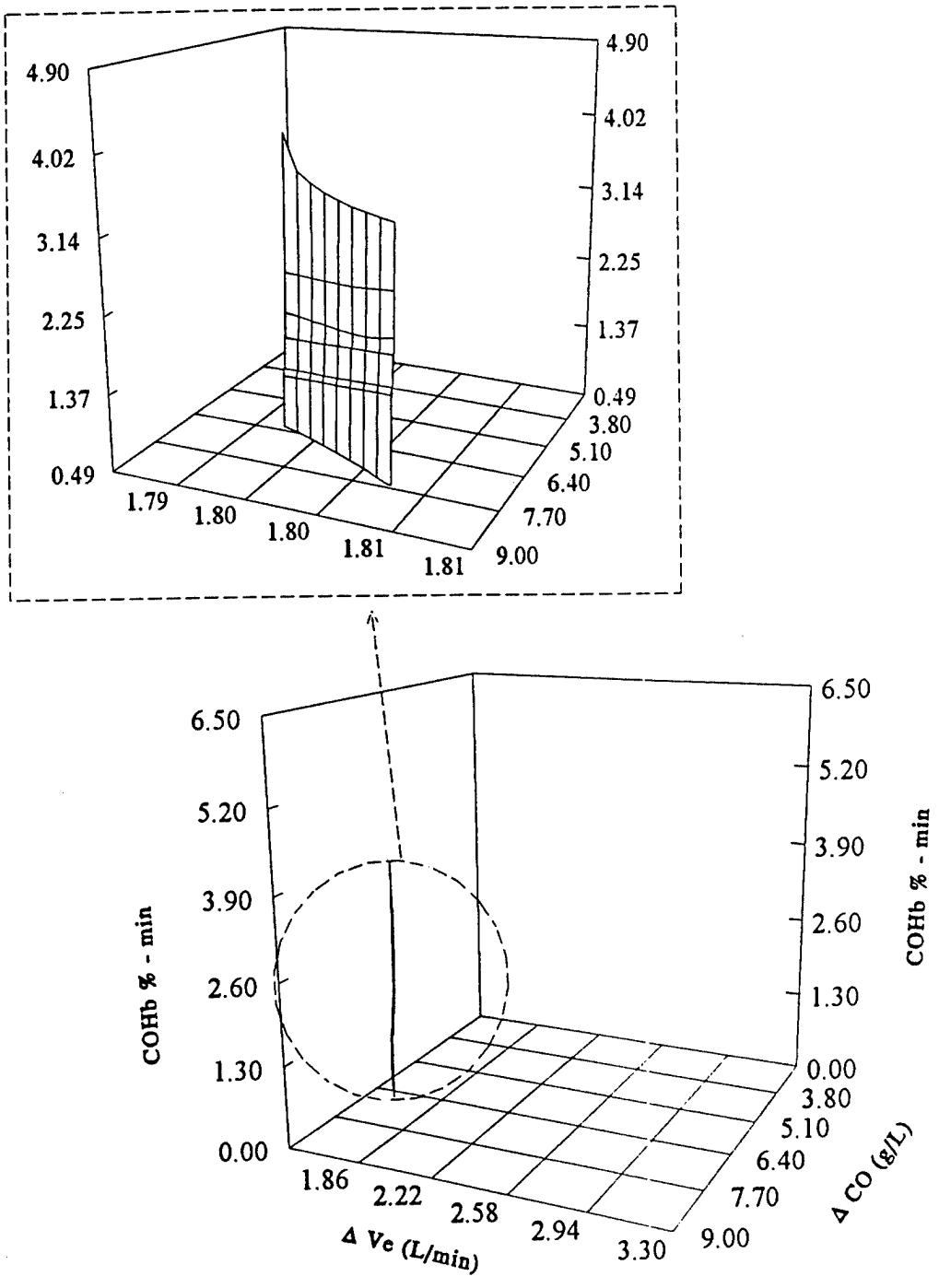

Figure 22. Cumulative carboxyhemoglobin formation - 0.7 m^3 chamber at 80 g/m^3.

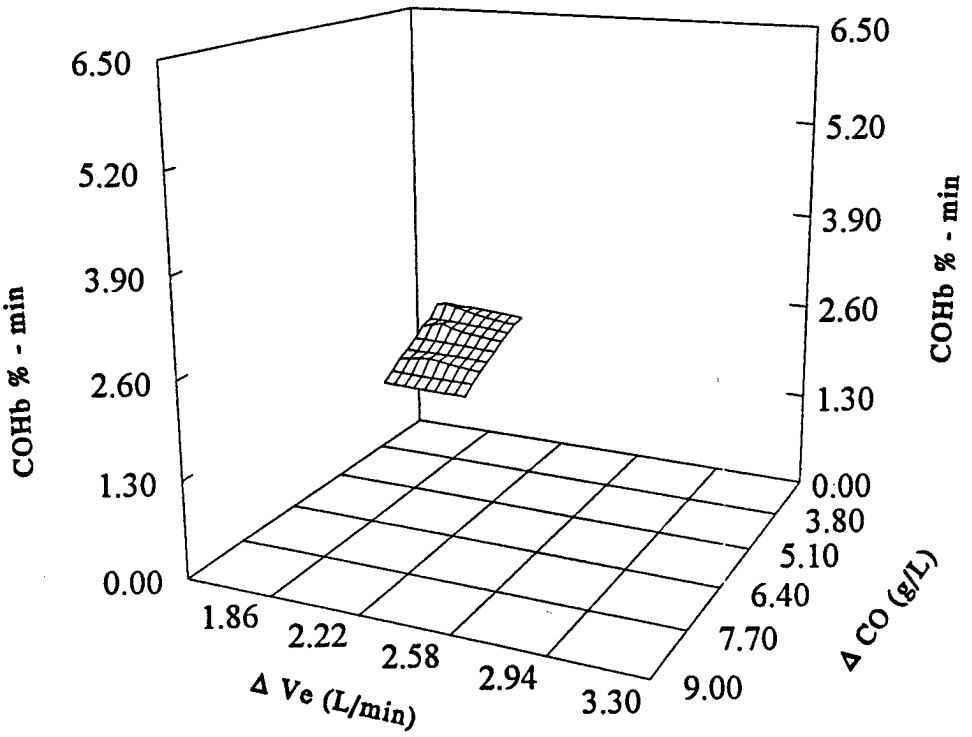

Figure 23. Cumulative carboxyhemoglobin formation - 56 m^3 chamber at 50 g/m^3.

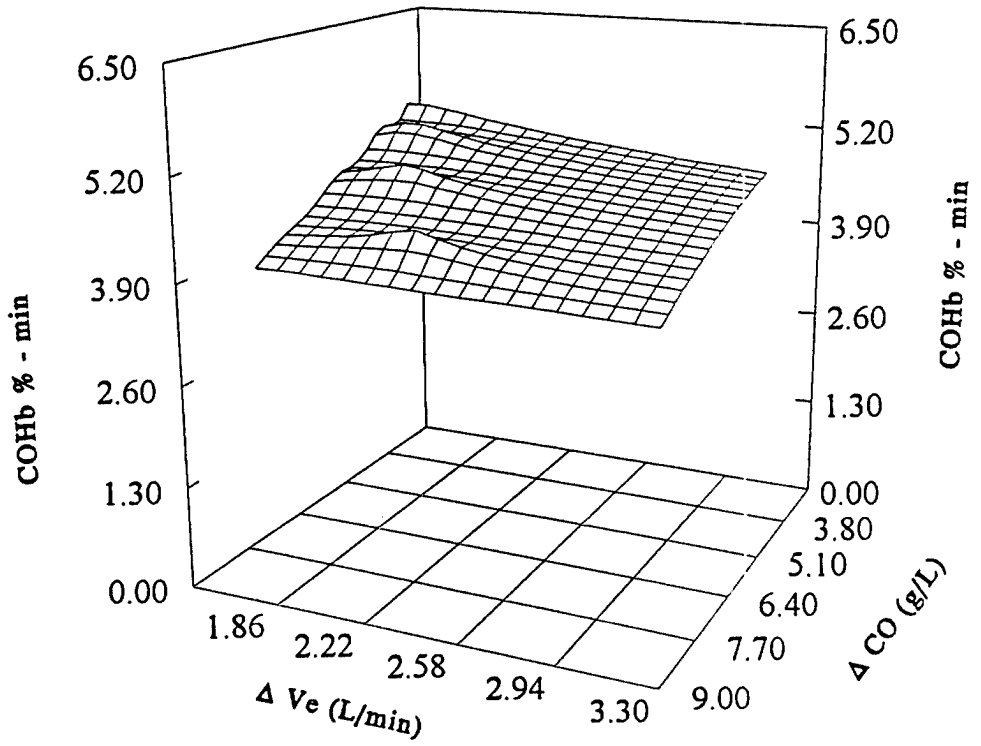

Figure 24. Cumulative carboxyhemoglobin formation - 56 m^3 chamber at 80 g/m^3.